Arab Academy for Science and Technology and Maritime Transport

College of Engineering and Technology

Department of Electrical and Control

Applying an Intelligent Technique for Identification of Abnormal Conditions within Transformers

Submitted by

Eng. Ahmed Sayed Abd El-Hamid Awad

A thesis submitted to the Faculty of Engineering, AASTMT, in partial fulfillment of the requirements for the M.Sc. degree in Electrical and Control Engineering

Supervised by

Prof. Dr. Rania Metwally El-Sharkawy

Electrical and Control Engineering Department

Arab Academy for Science and Technology and Maritime Transport

Cairo 2015

ARAB ACADEMY FOR SCIENCE, TECHNOLOGY AND MARITIME TRANSPORT

College of Engineering and Technology

Applying an Intelligent Technique for Identification of Abnormal Conditions within Transformers

By

Eng. Ahmed Sayed Abd El-Hamid Awad

A Thesis Submitted in partial fulfillment to the Requirements for the Master's Degree in Electrical & Control Engineering

Prof. Dr. Rania Metwally El-Sharkawy
Supervisor

____

Prof. Mohamed Badr
Examiner

____

Prof. Yasser Galal
Examiner

____

ACKNOWLEDGEMENT

First and foremost, I would like to thank God, who gives us the power and hope to succeed. The following document summarizes a year's worth of effort, frustration and achievement. However, there are several people with whom I am indebted for their contribution in the research, study and dissertation of this thesis.

My deepest and sincere gratitude goes to my supervisor, Prof. Dr. Rania El-Sharkawy, for giving me the chance for further studies in the field of power engineering and explore the challenging world of research. Particularly for persistent inspiration, valuable guidance, tremendous support and angelic patience. Her inexhaustible pursuit, enthusiasm and high demand of excellence towards research made a very profound impression and set up a model for me to follow. Not only being excellent supervisor, she is also as understanding and considerate as my own mother. Without her, I would not be here today, in both the academic world and the real world. It is really a pleasure to have Prof. Dr. Rania as my supervisor.

I would like to thank my father, mother, and brother for giving me their full support, understanding and patience over the years. Without their support, I would not have been able to finish my study program.

Last but not least, many thanks go to all my professors and friends. Especially Dr. Eman Beshr which was of enormous help. Also a thank you for Dr. Mohamed Gamal, Eng. Hatem Seoudy, Eng. Karim Ibrahim, Eng. Ibrahim kassem, Eng. Alaa, and Eng. Mohamed El-Adly who helped me and encouraged me when I needed it the most. Their friendship and support is one of my greatest assets.

ABSTRACT

In recent times, power transformers are among the most critical of assets for electric utilities in the power system. Frequency response analysis (FRA) is a powerful diagnoses method which is used to detect mechanical deformations within power transformers. The determination of FRA for any transformer can be made by its material properties and geometry. FRA is considered as the fingerprint of the transformers. The main drawback of the FRA, in addition to its being an off-line tool, is that it depends on graphical analysis. So, there is requires an expert to analyze this graphical results to show the presence of failure within transformer windings. Hence, there is increases the need for an online monitoring tool to assess the internal condition of transformers.

The present work is aimed to introduce novel online technique to detect the internal faults within a power transformer by constructing (ΔV- I_{in}) locus diagram. The advantage of this technique is the use of the existing measuring devices attached to any power transformer to monitor the input, output voltage in addition to the input current. Thus, it can be utilized as an online monitoring technique. Any deformation or displacement in the transformer winding can cause change in the circuit parameters and response. The changes can be detected using the proposed technique. This technique requires a reference response which is generated during commissioning of the transformer to detect these changes.

The purpose of this thesis is to first, simulate the several different types of insulation failure, and second to identify and classify the fault within transformer windings utilizing an intelligent technique. To achieve these goals, the proposed winding model and five types of insulation failures that are apt to occur in power transformers are implemented in power simulation (PSIM). The transformer parameters have been calculated from the practical design data of a 3 MVA, 33/11 kV, three-phase, 50 Hz, ONAN, Dy11 power transformer.

Contents

ACKNOWLEDGEMENT III
ABSTRACT IV
Contents V
LIST OF TABLES VII
LIST OF FIGURES VIII
LIST OF Symbols X
LIST OF ABBREVIATIONS XI
1. INTRODUCTION 1
1.1. Background 1
1.2. Problem Formulation 1
1.3. Aim or Research Motivation 2
1.4. Outline of the thesis 3
2. BACKGROUND INFORMATION 5
2.1. Introduction to power transformers 5
2.2. Classification of transformer failure 7
2.3. Offline and online transformer winding diagnosis techniques 10
2.3.1. Offline techniques 10
2.3.1.1. Visual inspection (VI) 10
2.3.1.2. Short circuit impedance (SCI) 10
2.3.1.3. Transfer function methods (FRA/LVI) 10
2.3.1.4. Leakage reactance test 11
2.3.1.5. Ratio test 11
2.3.1.6. Winding resistance test 11
2.3.2. Advanced online techniques 12
2.3.2.1. Vibration method 12
2.3.2.2. Communication method 12
2.3.2.3. Current deformation coefficient method 12
2.3.2.4. Ultrasonic method 13
2.4. Artificial neural networks. 13

2.4.1. Neural networks introduction. 13
2.4.2. Learn vector quantization (LVQ). 15
2.4.3. Probabilistic Neural Network 18
3. MODELING AND SIMULATION 19
3.1. Introduction 19
3.2. Adopted diagnostic technique 20
3.3. Undertaken transformer model 25
3.4. Simulation structure 27
3.5. Simulation result 28
3.5.1. Healthy condition 28
3.5.2. Fault conditions 29
3.5.2.1. PDF within transformer winding 29
3.5.2.2. IDF within transformer winding 32
3.5.2.3. SEF within transformer winding 33
3.5.2.4. SHF within transformer winding 34
3.5.2.5. ADF within transformer winding 35
4. FAULT DISCRIMINATION 37
4.1. Visual discrimination 37
4.2. Fault discrimination using traditional techniques 38
4.2.1. Image pixels discrimination 38
4.2.2. Mean square error 38
4.3. Feature extraction 39
4.4. Computational discrimination 42
5. ARTIFICIAL INTELLIGENCE BASED FAULT IDENTIFICATION 45
5.1. Conventional fault classification technique (if-condition based image comparator). 46
5.2. Results and discussion 49
CONCLUSION 62
REFERENCES 63
APPENDIX 66

LIST OF TABLES

Table 2.1: Standardized test voltages for rated voltages………………………………………. 6
Table 2.2: Thermal faults categories………………………….. 7
Table 2.3: Causes of transformer failure……………………………………………………... 8
Table 2.4: Transformer Component Failures…………………………………………………... 9
Table 4.1: Effect of faults on locus area and axis rotation……………………………………... 37
Table 4.2: Ellipse axes output………………………………………………………………………. 40
Table 4.3: General ellipse features for healthy condition……………………………………… 41
Table 4.4: Effect of different faults on locus area and axis rotation…………………………... 43
Table 5.1: Confusion matrix showing identification accuracy of train, validation and test data points……………………………………………………………………………… 59

LIST OF FIGURES

Figure 1.1:	**Flow Chart of Thesis Work Steps…………………………………………………**	**4**
Figure 2.1:	**Failures for large power transformers with on-load tap changers………………..**	**9**
Figure 2.2:	**A single mathematical neuronal model…………………………………………..**	**13**
Figure 2.3:	**LVQ neural network structure…………………………………………………**	**15**
Figure 2.4:	**The model of LVQ neural network……………………………………………..**	**16**
Figure 3.1:	**(a) Per-unit equivalent circuit of the transformer. (b) Vector diagram…………..**	**21**
Figure 3.2:	**Graphical illustration of V-I relationship……………………………………..**	**24**
Figure 3.3:	**Equivalent circuit of a single transformer winding………………………………**	**25**
Figure 3.4:	**Algorithm for developed simulation……………………………………………**	**27**
Figure 3.5:	**Locus diagram of 3MVA, 33/11KV transformer power in healthy condition…….**	**28**
Figure 3.6:	**PD pulse waveforms using Gaussian pulses of similar current magnitude value but different pulse width………………………………………………………….**	**30**
Figure 3.7:	**PD pulse waveforms using the double exponential pulse equation where ($\alpha = 10^8\, sec^{-1}, \beta = 8 * 10^7 sec^{-1}$)………………………………………………...**	**30**
Figure 3.8:	**The (ΔV - I_{in}) locus for injecting PD pulse at nodes 44 and 48 compared to the healthy locus……………………………………………………………….**	**31**
Figure 3.9:	**Effect of IDF on the (ΔV- Iin) locus…………………………………………….**	**32**
Figure 3.10:	**Series fault at disc one…………………………………………………………...**	**32**
Figure 3.11:	**Effect of SEF on the (ΔV- Iin) locus…………………………………………….**	**33**
Figure 3.12:	**Shunt fault at disc one…………………………………………………………...**	**34**
Figure 3.13:	**Effect of SHF on the (ΔV- Iin) locus……………………………………………**	**34**
Figure 3.14:	**Effect of ADF on the (ΔV- Iin) locus……………………………………………**	**35**
Figure 4.1:	**Comparison of the effect of each fault on the (ΔV- Iin) locus (40 discs)…………..**	**36**
Figure 4.2:	**Uniform plan wave……………………………………………………………**	**38**
Figure 4.3:	**General ellipse…………………………………………………………………….**	**39**
Figure 4.4:	**Effect of faults on locus area…………………………………………………….**	**42**
Figure 4.5:	**Effect of faults on locus angle of rotation……………………………………**	**42**
Figure 5.1:	**Block diagram representation of fault identification scheme……………………**	**44**
Figure 5.2:	**Logic flow diagram for identification of fault characteristics……………………...**	**46**
Figure 5.3:	**The five classes according to two features (area and theta) …..…………………..**	**48**
Figure 5.4:	**The five classes according to two features (area and circumference)……………...**	**48**
Figure 5.5:	**The five classes according to two features (area and semi major axis length)……**	**49**
Figure 5.6:	**The five classes according to two features (area and semi minor axis length)……**	**49**
Figure 5.7:	**The five classes according to two features (area and focus)………………………..**	**50**
Figure 5.8:	**The five classes according to two features (area and first eccentricity)…………...**	**50**

Figure 5.9: The five classes according to two features (area and second eccentricity)……….. 51
Figure 5.10: The five classes according to two features (area and ratio between eccentricities). 51
Figure 5.11: The five classes according to two features (area and flattering)………………….. 52
Figure 5.12: The five classes according to two features (area and average value of load voltage)…………………………………………………………………………….. 52
Figure 5.13: The five classes according to two features (area and root mean square value of load voltage)………………………………………………………………………. 53
Figure 5.14: The five classes according to two features (area and average of the absolute value of load voltage)…………………………………………………………...…. 53
Figure 5.15: Fault identification flow chart…………………………………………………….. 54
Figure 5.16: Errors in layer one classification of validation data……………………………... 55
Figure 5.17: Actual and predicted locus when we test the algorithm at different fault locations SEF type………………………………………………………………… 57
Figure 5.18: Actual and predicted locus when we test the algorithm at different fault locations IDF type………………………………………………………………… 57
Figure 5.19: Actual and predicted locus when we test the algorithm at different fault locations ADF type……………………………………………………………….. 58
Figure 5.20: Actual and predicted locus when we test the algorithm at different fault locations PDF type………………………………………………………………... 58
Figure 5.21: Actual and predicted locus when we test the algorithm at different fault locations SHF type………………………………………………………………... 59

LIST OF Symbols

ΔV	**Voltage; $\Delta V = V_{in} - V_{out}$**
I_{in}	**Input current**
δ	**Power angle**
γ	**Load impedance phase angle**
φ	**Phase shift between i_2 and v_2**
Φ	**Angle between i_1 and V_2**
R	**Resistance per disc**
L	**Total inductance per disc**
C_s	**Series capacitance per disc**
C_{sh}	**Ground capacitance per disc**
S	**Total number of sections**
I_{max}	**Magnitude of the peak current in (amperes)**
t	**Time in (seconds)**
σ	**Pulse width**
α, β	**Time coefficients (reciprocal seconds)**
a	**Ellipse major axis length**
b	**Ellipse minor axis length**
A	**Ellipse semi- major axis length**
B	**Ellipse semi- minor axis length**
θ	**Angle between the semi-major axis and the horizontal axis**
f	**Ellipse focus**
e	**First ellipse eccentricity**
e'	**Second ellipse eccentricity**
g	**Ellipse flattering**
$A_{ellipse}$	**Ellipse area**
$C_{ellipse}$	**Ellipse circumference**
$V_{L_{av}}$	**Average value of load voltage**
$V_{L_{rms}}$	**Root mean square value of load voltage**
$V_{L_{abs}}$	**Absolute of the average value of load voltage**

LIST OF ABBREVIATIONS

DGA	**Dissolved Gas Analysis**
FRA	**Frequency Response Analysis**
ANNs	**Artificial neural networks**
PSIM	**Power simulation**
AC	**Alternating current**
BIL	**Basic insulation levels**
IEC	**International Electro-technical Commission**
U.S.A	**United States of America**
VI	**Visual inspection**
SCI	**Short circuit impedance**
FFT	**Fast Fourier transform**
TTR	**Transformer turns ratio**
MAMD	**Mean absolute magnitude distance**
MAPD	**Mean absolute phase distance**
CDC	**Current deviation coefficient**
VFTO	**Very fast transient over-voltages**
FTO	**Fast transient over-voltages**
ONAN	**Oil Natural Air Natural**
PDF	**Partial Discharge fault**
IDF	**Inter disk fault**
SEF	**Series short circuit**
SHF	**Shunt short circuit**
ADF	**Axial Displacement fault**
PD	**Partial discharge**
RMS	**Root mean square**
BPANN	**Back propagation artificial neural network**
RBF	**Radius function network**
PNN	**Propagations neural network**
SOM	**Self-organizing map**
LVQ	**Learn vector quantization**
FRFD	**Frequency response fault diagnoses**

CHAPTER ONE

1. INTRODUCTION

1.1. Background

A power transformer is mainly used when there is a need for a voltage transformation, and it is used for transmission and distribution of electric power systems. The electric energy is transferred between different electrical circuits in transformer by the use of electromagnetic induction. Power transformers are usually expensive and require through maintenance and condition monitoring to maintain the continuity of supply.

1.2. Problem Formulation

Power transformers play very important role in the reliable operation of power systems. They are designed to function at supply frequency. In the event that a failure occurs in service, the impact can be far reaching. Not only can extended outages occur, but costly repairs and potentially serious injury or fatality can result. The aging transformer population increases the likelihood of failure, this poses significant a risk for utilities and other power network stakeholders as the impact of an in-service transformer failure can be catastrophic. Therefore, maintaining the integrity of insulation within the power transformer is crucial. Thus, there is an increasing need for better diagnostic and monitoring tool to assess the internal condition of transformers.

Several diagnostic methods have developed a long time ago as a response to the need for condition assessment. Among these, Dissolved Gas Analysis (DGA) and Frequency Response Analysis (FRA) have emerged as the industry standard tests for assessing the condition of the transformer insulation / oil and the integrity of the winding structure, respectively. FRA is a powerful method which is used to detect mechanical deformations within power transformers in recent times. The FRA of a transformer is determined by its geometry and material properties, and it can be considered as the transformer's fingerprint. If there are any mechanical changes in the transformer, for example if the windings are moved or distorted, its fingerprint will also be changed so, mechanical changes in the transformer can be detected. In the FRA test, the transformer is taken out of service and a signal is applied to one winding terminal and the response is measured at another terminal [1]. The main drawback of the FRA, in addition to its being an off-line tool, is that it depends on graphical analysis i.e., an expert is required to analyze the results to show if the failure is present or not. Hence, there is a need for an online monitoring tool to assess the internal condition of transformers. Further modifications are investigated to apply the FRA test online [2].

In the last decade, some researchers had proposed several different computer aided techniques for classification of series and shunt insulation failures in transformer winding [3, 4]. Moreover, correlation technique in the frequency domain has been applied to localize the occurrence of partial discharge in 10 section lumped parameter transformer winding model [5].

Nevertheless, the platform is still open for the application of computer-aided diagnostic techniques for the assessment of the proper operation and the integrity of insulation within power transformer.

1.3. Aim or Research Motivation

The present thesis is aimed to simulate, analysis, and discriminate five types of insulation failure which may be produced after the offline impulse test that is routinely carried out on power transformers [1]. The technique is introduced to detect the internal faults within a power transformer by contracting (ΔV- I_{in}) locus diagram. The advantage of this technique is the use of the existing measuring devices attached to any power transformer to monitor the input, output voltage in addition to the input current. Thus, it can be utilized as an online monitoring technique.

This thesis also present two techniques to identify and classify the insulation failure within a power transformer based on developed code and artificial neural networks (ANNs). The proposed (ΔV- I_{in}) locus can be plotted every cycle (20 ms based on a 50-Hz network) and compared with the healthy locus using the developed code to immediately identify any changes. Hence, the fault is located along the winding of the transformer. The proposed technique is easy to be implemented and automated so that the requirement for expert personnel can be eliminated and early warning for the transformer condition obtained.

1.4. Outline of the thesis

The main concern in this thesis is directed to study the diagnosis in power transformers and propose a new strategy for the classification of the abnormality conditions in transformer windings. The following points are covered in this work:

1. Present a comprehensive literature survey about the addressed topic.
2. Select and simulate a suitable transformer for this study using power simulation (PSIM) software.
3. Develop an online diagnosis technique to present the current state of the transformer.
4. Develop a new expression of the (ΔV- I_{in}) locus diagram that is used in the diagnosis study.
5. Investigate the effect of different types of abnormal conditions within the simulated transformer by constructing (ΔV- I_{in}) locus diagram for the suitable transformer in healthy and faulty conditions.
6. Discriminate different types of insulation failure which may be produced on power transformers according to visual inspection and discrimination using feature extraction.
7. Develop an intelligent fault classification and localization technique using MATLAB.
8. Demonstrate results and conclusions.

Figure 1-1 shows all the processing stages utilized in this thesis to classify and locate the different types of failures apt to occur within the transformer windings.

This thesis focuses on the identification and classification of the insulation failure in the transformer windings using intelligent computational techniques that can be readily applied to online measurements. This thesis starts with a brief introduction about the mechanical failure problem and the research motivation. The second chapter is dedicated to overview for the power transformer and its reasons of failure and also discusses offline and online available transformer winding deformation diagnostic methods. The third chapter introduces an adopted diagnostic technique, the undertaken transformer model and discusses the simulation of the utilized power transformer and also studies and analyses the fault types. The fourth chapter.

The fourth chapter starts with the visual inspection of fault discrimination techniques applicable to transformer winding, and then details a developed algorithm (computational discrimination technique) used for fault discrimination within transformer winding utilizing feature extraction according to circuit model to identify the type of the fault in the transformer. The fifth chapter introduce the feature identification and location methods utilizing the Learn vector quantization (LVQ) algorithm.

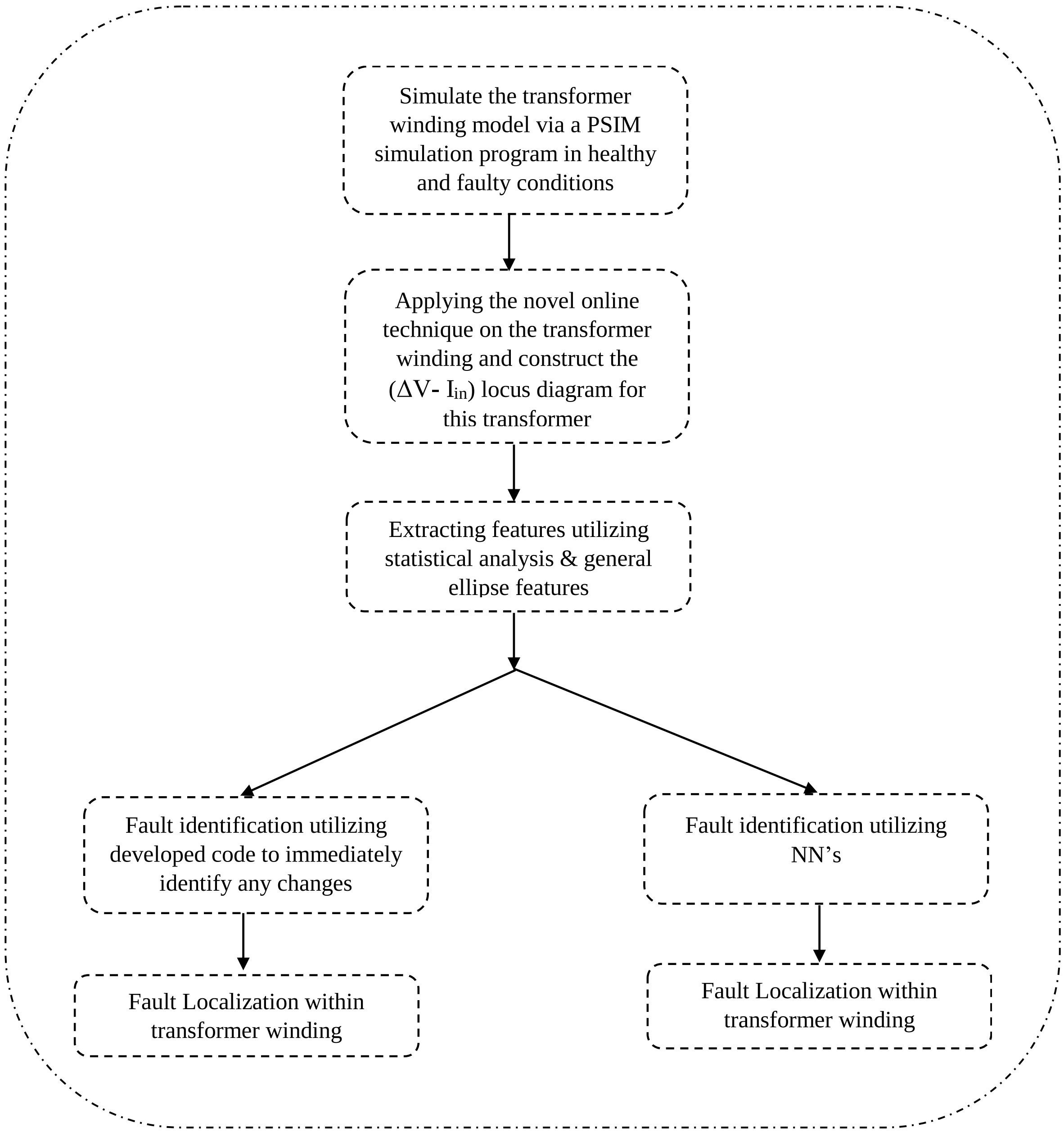

Figure 1-1 Flow Chart of Thesis Work Steps

CHAPTER TWO

2. BACKGROUND INFORMATION

2.1. Introduction to power transformers

In AC power systems, power transformers are among the most crucial physical assets in a power system in terms of their capital cost, network impact and cost due to unexpected failure.

A power transformer comprises of two or more windings that are coupled through a common magnetic core. A time-varying flux created by one winding induces voltages in all of the other windings. Laminated iron core, two or more windings, an insulation medium, a tank, bushing and accessories represent the main components of any transformer. Transformers can be categorized into different types according to different criteria. For example; depending on the construction of the core, transformers can be categorized as Core-type transformers and Shell-type transformers. In core-type transformers, the windings are wrapped around two sides of a sample rectangular window iron core; while in shell-type transformers, the windings are only wrapped around the center leg of a three-legged iron core. Also, with a particular point of view about the insulation medium, transformers fall into two categories:

- Dry type transformers: If the core and coils are in a gaseous or dry compound insulation.
- Fluid-filled transformers: this type of transformers have the core and coils impregnated with an insulating fluid and immersed in the same insulation medium.

An iron core is used because of its high relative permeability. As a result of its higher relative permeability, a smaller magnetizing current is required as compared to a non-ferromagnetic core. Furthermore, the iron core is usually laminated in order to minimize eddy current losses, which are generated in the core by the time varying magnetic flux.

The windings are usually made of copper or aluminum. The winding conductors may be either wires or sheets. Successive layers are insulated by sheets of insulation. Ceramic bushings are used to isolate the windings from grounded structures of the transformer such as the oil tank. Transformers with increasingly larger voltages require increasingly longer bushings to prevent an external flashover. Mineral oil is typically used as insulation medium. It is also used to cool the transformer.

The insulation must be capable of withstanding voltages greatly exceeding the rated winding voltages. Voltages must larger than the rated values can appear across the windings of the transformer during network transients. Such as switching operations, lightning strikes, short circuit faults, and fluctuations in the load. Table 2.1 shows the insulation levels for different voltage ratings, which are defined as the values of the required test voltages [6]. BIL, that is basic insulation levels, are given in the column 3 and column 7 for Europe and North America respectively.

Table 2.1 Standardized test voltages for rated voltages

Coordination of Insulation according to IEC Publication 71, 1972						
European practice and other countries				U.S.A. and Canada		
Rated voltage V_m*	Test voltage 50 Hz, 1 min	Lightning impulse voltage 1.2/50 µsec	Switching surge voltage 250/2500 µsec	Rated voltage	Test voltage 60 Hz, 1 min**	Lightning impulse voltage 1.2/50 µsec
KV in RMS	KV in RMS	KV in peak	KV in peak	KV in RMS	KV in RMS	KV in peak
3.6	10	40		4.76	19	60
7.2	20	60		8.25	26	75
12	28	75		15	36	95
17.5	38	95		15.5	50	110
24	50	125		25.8	60	125
36	70	170		38	80	150
100	185	450		100	185	450
145	275	650		145	275	650
175	325	750		175	325	750
245	460	1050		254	460	1050
300	380	1050	850			
362	450	1175	950			
420	520	1425	1050			
525	620	1550	1175			
765	830	2100	1425			

Note:

* V_m is the maximum service voltage of the network between phases.

**Test voltage is the phase voltage.

Outages due to power transformer failure cost the company money not only in replacement or repair, but also in buying power from other companies to supply their customers. These costs can quickly grows into millions of dollars in just a few days. A case study mentioned [7], estimated the failure of a 520MVA transformer to reach approximately US$18 Million in just 8 days.

2.2. Classification of transformer failure

Generally, transformer failures may be caused by a multitude of reasons. The literature review over the last several decades on transformer failure have different ways to categorize the causes of transformer failures.

One of these ways classified the transformer failure causes into two categories as "**internal causes**" and "**external causes**". Internal causes are due to the internal faults that happen inside the tank such as: Short circuit between windings or turns, Insulation deterioration, Loss of winding clamping, Overheating, Oxygen, Moisture, Solid contamination in the insulating oil, Partial discharge, Design & manufacture defects or internal winding resonance. While, external causes are due to external faults that related to bushing, leads and accessories that are outside the tank, and may be caused by system switching operations, lightning strikes, system overload and system fault (short circuits). The internal faults can be split further to thermal faults and electrical faults. Generally, Transformers overheating due to thermal faults. According to the severity of the faults, thermal faults are often divided into four categories listed in table 2.2. Under high electric field electrical faults cause the degradation of the insulation. According to the degree of discharge intensity, electric faults are further divided into partial discharge, spark discharge and arc discharge.

Table 2.2. Thermal faults categories

Thermal fault category type	temperature
Slight temperature overheating	less than 150°C
Low temperature overheating	150-300°C
Medium temperature overheating	300-700°C
High temperature overheating	More than 700°C

Another way for fault classification ways is based on circuitry. According to "circuitry", failures can also be split into two categories as "**structure of main body**" and "**fault location**". By structure of the main body of the transformers, failures can be divided into winding faults (or electric faults), core faults (or magnetic faults), oil faults (or oil path faults), and accessory faults; by fault location, failures can be divided into insulation faults, core faults and tap-changer faults, etc. All of the above failures can either reflect thermal failures, electric failures or both. A survey listed the percentage of several reasons of transformer failures (internal and external reasons) as shown in Table 2.3 was conducted by Hartford Steam Boiler over the last several decades on thousands of transformer failures [8].

Table 2.3. Causes of transformer failure

Failure percentage per year	1975	1983	1998	winding movement evident
Lightening surges	32.3 %	30.2 %	12.4 %	✓
Line surges / External short circuit	13.3 %	18.6 %	21.5 %	✓
Poor workmanship-Manufacturer	10.6 %	7.2 %	2.9 %	✓
Insulation deterioration	10.4 %	8.7 %	13 %	×
Overloading	7.7 %	3.2 %	2.4 %	×
Moisture	7.2 %	6.9 %	6.3 %	×
Inadequate Maintenance	6.6 %	13.1 %	11.3 %	✓
Sabotage, Malicious Mischief	2.6 %	1.7 %	0 %	×
Loose Connections	2.1 %	2.0 %	6.0 %	✓
All others	6.9 %	8.4 %	24.2 %	--

As shown in Table 2.3., the main reasons of transformer failures are lightning surges, switching surges, insulation deterioration and inadequate maintenance. Another international survey shows the percentage of failures related to the structural components (fault location) of the transformers was conducted by the CIGRE Working Group [17], as shown in Figure 2.1. Figure 2.1. Show that, the main components that cause failures in large power transformers are on-load tap changers, windings, and tank/fluid. An article [18] in Electricity Today tabulates transformer failures by their components as given in Table 2.4.

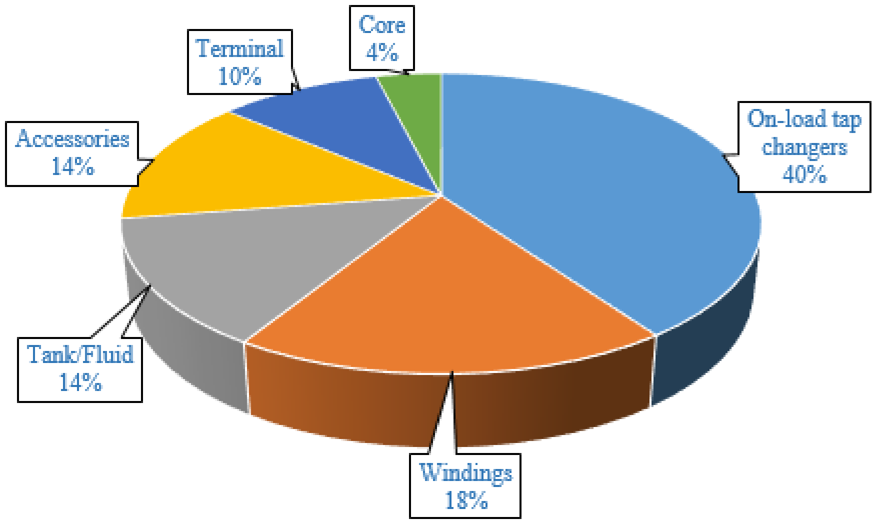

Figure 2.1. Failures for large power transformers with on-load tap changers

Table 2.4. Transformer Component Failures

Transformer component	**Failure percentage**	**Insulation System**
High Voltage Windings	48%	Yes
Low Voltage Windings	23%	Yes
Bushings	2%	Yes
Leads	6%	No
Tap Changers	0%	No
Gaskets	2%	No
Other	19%	No
Total	100%	--

2.3. Offline and online transformer winding diagnosis techniques

Major diagnostic methods which are employed by utilities and researchers include off and on-line methods where are introduced as diagnostic tools by [9, 14] as follows:

2.3.1. Offline techniques

2.3.1.1. Visual inspection (VI)

In this test; the transformer has to be taken out of service, and opened up to be inspected after drained. The clamps, windings and insulation condition can then be inspected to determine if there are any noticeable problems. It requires expert to carry out inspections and can lead to long out of service times for the transformer, which is undesirable. This method is the most reliable method to determine the winding condition, and it is likely to be retained only as a final verification when a less invasive method detects the presence of critical damage.

2.3.1.2. Short circuit impedance (SCI)

SCI method is usually used for transformer winding deformation detection. Measured SCI of a power transformer can be compared to the value that appears at the nameplate or factory test results. It is employed to detect winding movement that may have occurred since the factory tests were performed. To conduct this test, the low voltage winding terminals have been short-circuited to each other and the input current voltage and power are measured. Changes of more than ±3% of the SCI should be considered significant [15].

2.3.1.3. Transfer function methods (FRA/LVI)

Transfer function is basically a way of describing a system behavior. Transfer function method is increasingly used in the diagnostics of electric power equipment, especially for the identification of winding integrity in transformers [16-18]. Transfer function measurement has been developed based on two popular methods. The first one applies in time domain while the second one is concentrated on frequency domain. Frequency domain measurement is performed by injecting a swept sinusoidal waveform within a predetermined frequency band. Some researchers believe that acceptable and judicable result would be taken in between 10 Hz and 1 MHz [19] while the others have recommended max extended frequency response measurement up to 10 MHz [20]. In time domain method, an impulse voltage waveform is injected into the test object and time domain response measured through test object output. Once the time domain measurement data is at hand, transfer function in frequency domain could be determined by using Fast Fourier transform (FFT) technique. Generally, the purpose of both methods is to excite the natural frequencies of the test object.

2.3.1.4. Leakage reactance test

The short circuit impedance test set-up can also be used to calculate the leakage reactance of the transformer. If the winding has expanded, the leakage reactance would increase as a consequence. This method is sensitive to certain types of distortion only, namely distortion that results in increased distance between the primary and secondary coil. It does not pick up distortions such as twisting of windings and is ineffective at high frequencies due to the skin effect.

2.3.1.5. Ratio test

The winding ratio test is an offline test that can be used to detect faulty winding conditions (short circuit or open circuit). The transformer voltage ratio is tested to ensure that the proper turns-ratio is present. This test determines the transformer turns ratio (TTR) of the number of turns in the high-voltage winding to that in the low-voltage winding. The ratio test shall be made at rated or lower voltage and rated or higher frequency. The tolerance for the ratio test is 0.5% of the winding voltages specified on the transformer nameplate.

2.3.1.6. Winding resistance test

The winding resistance test can be used to detect fraction of an ohm changes of the transformer winding. So, this technique requires highly sensitive equipment. Also, this test is an offline test. Any change in the geometry of the conductor would show up as a change in the winding resistance, this is the main idea in this test. For example, if the winding expands then the length of the winding would increase while the cross sectional area would decrease. This would cause an increase in the resistance of the winding. Generally, variations of more than 5% are considered indicative of damage.

2.3.2. Advanced online techniques

2.3.2.1. Vibration method

Transformer vibration can be considered to be repetitive movement of transformer inner parts that are covered by the transformer tank. This movement is done around a reference position. The reference position is where the transformer attains once it is out of service. Vibration might be interpreted by using parameters such as winding displacement, velocity and acceleration. Vibration testing involves the mounting of acoustic sensors on the tank wall of the transformer to sense the vibration of the transformer caused by the continuous magnetization and demagnetization of the core and windings. These acoustic signals form the signature for the winding. This method has the advantage of being an online method; however the externally mounted sensors are highly susceptible to vibration noise from the external environment. In addition, [21-23] have introduced an on-line method. These studies show that transformer tank vibration depends on voltage square and current square. Furthermore, studies reveal that winding vibration main harmonic component is 100 Hz when fundamental power frequency is 50 Hz. Therefore, transformer tank vibration has been recommended to be considered as an online transformer winding deformation diagnosis method.

2.3.2.2. Communication method

Communication method which is introduced in the literature [24-26] is applied based on scattering parameters. The magnitude and phase of scattering parameters for normal transformer winding are measured by several antennas as finger print. Proposed antennas could be placed outside or inside the transformer tank. In this method mean absolute magnitude distance (MAMD) and mean absolute phase distance (MAPD) are introduced as displacement indices. As has mentioned in [24-26], any kind of transformer winding deformation can cause abovementioned indices are altered and deformation detected.

2.3.2.3. Current deformation coefficient method

This method has been introduced by [27], and by using that a high frequency low voltage signal is applied to live power system line along with power frequency signal when the standard practices of connection are considered. The line-end and neutral-end high frequency currents are continuously measured using isolated precision current probes and digital filtering technique [27]. Associated capacitive reactance is changed due to the transformer winding deformation and this change is reflected in deviations of high frequency terminal currents from fingerprint. When these deviations are measured, the ratio of deviations at the two ends is calculated. Hence, current deviation coefficient (CDC) is introduced as justifiable relation.

2.3.2.4. Ultrasonic method

Ultrasound is a sound with a frequency greater than the upper limit of human hearing. In this method introduced in [28], an ultrasonic signal has been used as reference signal. The basis of this method concentrates on ultrasound reflection due to the non-matching acoustic impedance between oil and the winding.

2.4. Artificial neural networks.

2.4.1. Neural networks introduction.

ANNs have been around since the late 1950's, it was not until mid-1980 that algorithms became sophisticated enough for general applications.

ANNs are collections of mathematical models that emulate some of the observed properties of biological nervous systems and draw on the analogies of adaptive biological learning. The key element of the ANN paradigm is the novel structure of the information processing system. It is composed of a large number of highly interconnected processing elements that are analogous to neurons and are tied together with weighted connections that are analogous to synapses. A typical neuronal model is thus comprised of weighted connectors, an adder and a transfer function (Figure 2.2).

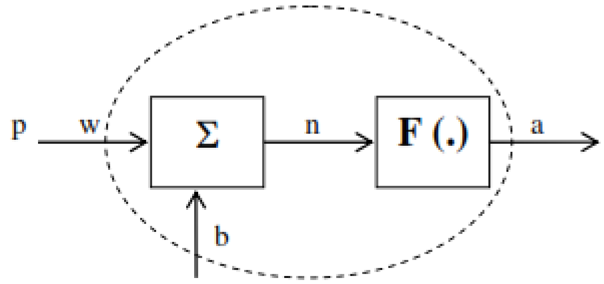

Figure 2.2. A single mathematical neuronal model

The basic relationship here is:

$$n = wp + b \tag{2.1}$$

$$a = F\,(wp + b) \tag{2.2}$$

Where:

a = network output signal

w = weight of input signal

p = input signal

b = neuron specific bias

F = transfer/activation function

n = induced local field or activation potential

Learning in biological systems involves adjustments to the synaptic connections that exist between the neurons. This is true of ANNs as well. Learning typically occurs by example through training, or exposure to a trothed set of input/output data where the training algorithm iteratively adjusts the connection weights (synapses). These connection weights store the knowledge necessary to solve specific problems. From equations 2.1 and 2.2, it can be seen that a simple neuron performs the linear sum of the product of the synaptic weight and input with the bias, which value is then passed through an activation or transfer function that limits the amplitude of the output of a neuron. Activation functions can take various forms ranging from hard limit, through pure linear to sigmoid and the choice of which to use depends on the desired output from the network and the characteristics of the system being modelled.

Typical and practical networks are normally multi-input and probably multi-layered and in such cases, the variables in equations 2.1 and 2.2 now take a different format with w being the matrix of weights and a, p and b representing vectors of their respective definitions.

1. Their building blocks are highly interconnected computational devices though the artificial neurons are much inferior to their biological counterparts.
2. The function of the network is determined by the nature of connection between the neurons.

ANNs are excellent at developing systems that can perform information processing similar to what our brain does. Some characteristics of biological networks include the following:

- They are non-linear devices
- They are highly parallel in processing, robust and fault tolerant
- They can easily handle imprecise, fuzzy, noisy and probabilistic information
- They can generalize from known tasks or examples.

ANNs attempts to mimic some or all of these characteristics by using principles from the nervous system to solve complex problems in an efficient manner.

There are several different types of ANN strategies used in PD recognition. They are:

Back-propagation NN, self-organizing feature map [29], learning vector quantization network [30]…etc.

2.4.2. Learn vector quantization (LVQ).

LVQ neural networks can be applied to multi-class classification problems. So, recently, LVQ networks are usually the choice where neural network based classifiers are used in field of diagnostic procedures. Feng Yan [31] found that LVQ networks is quite effective and superior to BP Neural Network in fault location in distribution network. Jianye Liu, Yongchun Liang, and Xiaoyun Sun [32] presented LVQ to analyze the fault of the power transformer, and it conclude that “the LVQ network a good classifier for the fault diagnosis of power transformer”.

LVQ network has simple network structure. Figure 2.3 show LVQ neural network that used in this work. It is composed by three layers of neurons; a first input layer, second competitive layer and third linear layer. In LVQ neural network, the competitive layer learn to classify input vectors into target classes chosen by the user while the linear layer transforms the competitive layers classes into the predefined target classifications. A weight value connect each neurons of input layer to all the neurons in the competitive layer. A different group of competitive neurons are connected with each output neuron. Connection weights value between competitive layer and output layer is always 1.

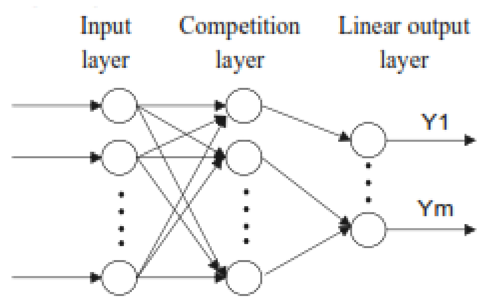

Figure 2.3. LVQ neural network structure

LVQ does not need to handle input vector for normalization and orthogonal. And it only needs to calculate the distance between input vector and competition layer directly. Therefore, it is easy to realize the category of fault [7]. The LVQ neural network model is shown in Figure 2.4.

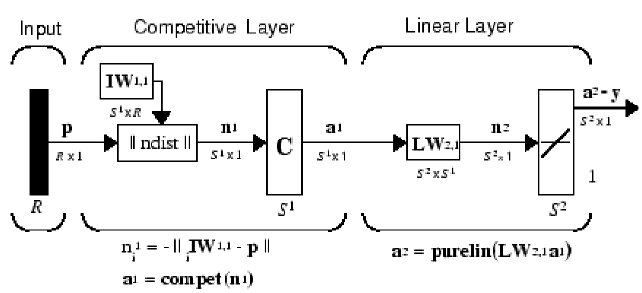

Figure 2.4. The model of LVQ neural network

We refer to the classes learned by the competitive layer as subclasses and the classes of the linear layer as target classes. Both the competitive and linear layers have one neuron per (sub or target) class. Each neuron in the competitive layer is assigned to a class, with several neurons often assigned to the same class. Each class is then assigned to one neuron in the linear layer. The number of neurons in the competitive layer S1 is always larger than the number of neurons in the linear layer S2. In the LVQ network, the input vector P with R neurons of the input layer will be given in by equation 2.3.

$$P = (p1, p2, p3 \dots p_R) \tag{2.3}$$

Input weights vectors that make the connection between input layer and competitive layer are

$$w^1 = \left(w_1^1, w_2^1, w_3^1 \dots w_{s^1}^1\right) \; w_\mathrm{i}^1 = \left(w_{\mathrm{i}1}^1, w_{\mathrm{i}2}^1, w_{\mathrm{i}3}^1 \dots w_{is^1}^1\right) \tag{2.4}$$

Where, i=1, 2 … s^1

The competitive layer input will be given in vector form by equation 2.5.

$$n^1 = -\begin{bmatrix} \|w_1^1 - p\| \\ \|w_2^1 - p\| \\ \vdots \\ \left\|w_{s^1}^1 - p\right\| \end{bmatrix} \tag{2.5}$$

Where w_i^1represents the input weight matrix, i denotes the corresponded neuron. The output of the competitive layer is given as follows.

$$a^1 = compet(n^1) \tag{2.6}$$

Therefore the neuron whose weight vector is closest to the input vector will output one, and the other neurons will output zero. Thus, the winning neuron indicates a subclasses, rather than a class as in competitive networks. There may be several different neurons (subclasses) that make up each class.

The linear layer in the LVQ network is used to combine subclasses into a single class which is done by the weight matrix w^2. The columns of w^2 represent subclasses, and the rows represent classes. w^2 has a single 1 in each column, with the other elements set to zero. The row in which the 1 occurs indicates which class the appropriate subclass belongs to, in other words,

$w_{\mathrm{ki}}^2 = 1$ Subclass i is a part of class k.

Weights vectors that make the connection between competitive layer and output layer are

$$w^2 = \left(w_1^2, w_2^2, w_3^2 \dots w_{s^2}^2\right) \ w_{\mathrm{j}}^1 = \left(w_{\mathrm{j}1}^2, w_{\mathrm{j}2}^2, w_{\mathrm{j}3}^2 \dots w_{js^1}^2\right) \quad (2.7)$$

Where, j=1, 2 … s^2

The output of the linear layer is.

$$a^2 = purelin(w^2 a^1) \quad (2.8)$$

LVQ learning in the competitive layer is based on a set of input/target pairs

2.4.3. Probabilistic Neural Network

Specht (1988, 1990) developed the probabilistic neural network (PNN). PNN is used to provide solution to pattern classification problems through an approach developed in statistics, called Bayesian classifiers. In Bayes theory, the relative likelihood of events as well as priori information to improve prediction is considered.

PNN uses a supervised training set to develop distribution functions within a pattern (middle) layer. In the recall mode, the developed functions are used to determine the likelihood of a given pattern being a member of a class or category with the criteria solely based on the closeness of the input feature vector to the distribution function of a class.

PNN has three layers. The input layer has as many elements as there are separable parameters needed to describe the objects to be classified. The middle layer organizes the training set such that each input vector is represented by an individual processing element. And finally, the output layer, also called the summation layer, has as many processing elements as there are classes to be recognized.

PNNs are simple on design and with sufficient data are guaranteed to generalize well in classification tasks. Training of the PNN is much simpler than with backpropagation. However, the pattern layer can be quite huge if the distinction between categories is varied and at the same time quite similar in special areas. In addition, PNNs are slower to operate in the recall mode as more computations are done each time they are called.

CHAPTER THREE

3. MODELING AND SIMULATION

3.1. Introduction

Transformer is one of the most important and costly equipment in power systems which converts energy from one potential side to another. Transformers represent a high capital investment in any substations at the same time as being a key element determining the loading capability of the station within the network. With appropriate maintenance, including insulation reconditioning at the appropriate time, the technical life of a transformer can be in excess of 60 years.

Transformer windings are treated as an inductance when it is incorporated in the power system computations (typically when transformer is a part of a power system network). When the behavior of transformer winding subjected to very fast transient over-voltages (VFTO), which causes some mechanical deformations, is to be studied, this assumption of lumped inductance does not hold well. So, for power flow studies or even short circuits studies its complex nature is represented as an inductance. However, for the purpose of diagnostics, such simplification cannot be made.

The Fast transient over-voltages (FTO) and VFTO or generally electromagnetic transients, are the main causes of transformer outages, have wavelengths which are comparable to the dimension of the winding. Hence, it is more appropriate to model the transformer winding as a distributed parameter transmission line for the study of very fast transients. The detailed transformer transient models can be employed during the design stage to predetermine those over-voltages. Using these models, the proper insulation can be designed.

There has been a great deal of research work done on transformer modeling [33]. Due to different purposes for the models, different types of transformer models have been constructed and used. Generally, Transformer models usually fall into one of two categories.

1. Black Box or “Terminal Model”.

2. Gray Box or “Physical Model”.

One is the Black Box or “Terminal Model”, which is necessary for the insulation coordination of power system and can be employed to evaluate the current and voltage wave shapes at the terminals of the transformer (i.e. provides the terminal characteristics of a transformer). The Black Box model is not necessarily related to a transformer internal condition and physical configuration. This type of model mainly describes the terminal performance and characteristics, and can be constructed by various methods (e.g., mathematical equations or network analysis (poles and zeros)).

The other type of transformer model is the Gray Box or physical model. The physical model can either model all parts of the transformer in great detail or can be constructed according to gross physical components such as the winding layers. These types of models use network equivalent parameters (resistances, inductances and capacitances) to construct the model and focus on the frequency range of interest. Transformer models can be classified as power frequency range, medium frequency range (kHz) or high frequency range (MHz). The Gray Box models can be used by designers to study the resonance behavior of transformer winding and the distribution of electrical stresses along the transformer windings. .The Gray Box models can be categorized as Lumped models and Transmission line models.

This thesis is studying what influence the transformer internal changes have on the (ΔV - I_{in}) locus signature changes. In the case of the monitoring, it is desirable to see small changes in the transformer so that any movement can be detected as early as possible. To model this situation, a terminal model is not suitable as it is mainly used for system performance studies rather than being focused on transformer internal condition changes. A detailed model is preferred, but detailed design information for a transformer is very difficult to obtain, as it needs detailed proprietary manufacturing design data that manufacturers do not want to divulge. A reduced model is more suitable for the work in this thesis.

3.2. Adopted diagnostic technique

In the present work, we use the novel online technique for diagnosis of power transformer faults by constructing the voltage - current (ΔV- I_{in}) locus diagram to provide a current state of the transformer, which have been previously detected. This technique relies on constructing locus diagram between I_{in} (X-axis) and ΔV (Y-axis) for the transformer under test. Basically, this relationship between ΔV and I_{in} represents an Ellipse [6]. The relationship of this locus can be derived using the 1- $\boldsymbol{\varphi}$ transformer equivalent circuit and its vector diagram shown in Figure 3.1.

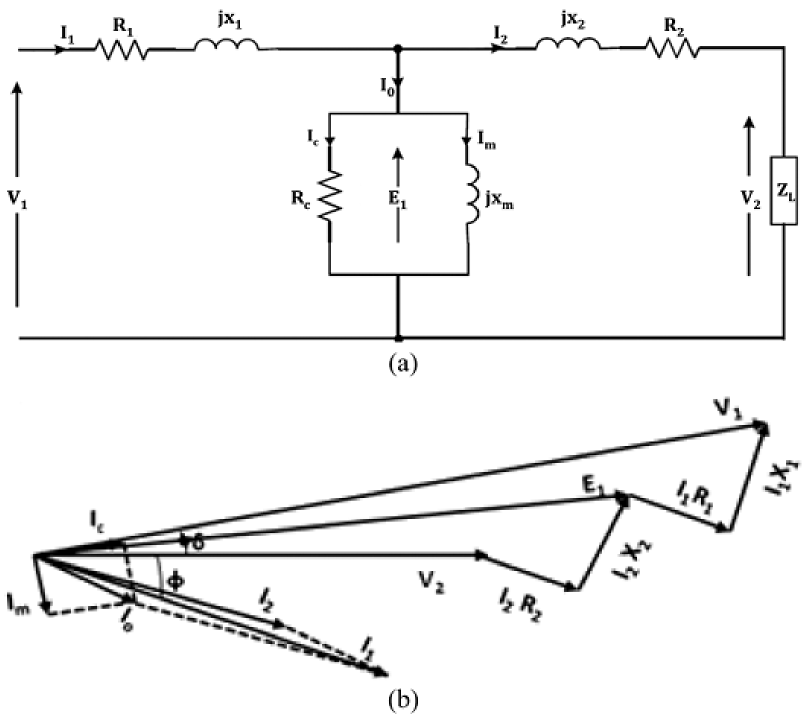

Figure.3.1. (a) Per-unit equivalent circuit of the transformer. (b) Vector diagram.

Let:

V_2 is a reference, δ is the power angle, and it is the phase shift between V_1 and V_2, which is normally small value, γ is the load impedance phase angle, φ represent the phase shift between i_2 and v_2, $\varphi = \gamma$. The phase shift between i_1 and v_2 is φ because the phase shift between i_1 and i_2 is approximately zero.

So,

$$v_1(t) = V_{m1}\sin(\omega t + \delta)$$

$$v_2(t) = V_{m2}\sin(\omega t)$$

$$i_1(t) = I_{m1}\sin(\omega t - \varphi)$$

For simplicity, assume that $V_{m1} = V_{m2} = V_m$.

Since (x − axis) → I_{in}(t) and (y − axis) → $\Delta V = v_{in} - v_{out}$

$$\therefore \mathrm{x} = \mathrm{i}_1(\mathrm{t}) = \mathrm{I}_{\mathrm{m}1}\sin(\omega\mathrm{t} - \varphi) \qquad (3.1)$$

$$\therefore y = v_1(t) - v_2(t) = V_m\{\sin(\omega t + \delta) - \sin(\omega t)\}$$

$$\therefore \mathrm{y} = 2\mathrm{V}_\mathrm{m}\cos(\omega\mathrm{t} + \tfrac{\delta}{2}).\cos\delta \qquad (3.2)$$

The Cartesian formula relating x and y can be obtained from parametric (3.1) and (3.2) by eliminating ωt as following. From equations (3.1) and (3.2), we get:

$$\omega t = \left\{\sin^{-1}(\frac{\mathrm{x}}{\mathrm{I}_{\mathrm{m}1}})\right\} + \varphi = \left\{\cos^{-1}(\frac{\mathrm{y}}{2\mathrm{V}_\mathrm{m}\cos\delta})\right\} - \frac{\delta}{2}$$

$$\therefore \left\{\cos^{-1}(\frac{\mathrm{y}}{2\mathrm{V}_\mathrm{m}\cos\delta})\right\} - \left\{\sin^{-1}(\frac{\mathrm{x}}{\mathrm{I}_{\mathrm{m}1}})\right\} = \left(\varphi + \frac{\delta}{2}\right)$$

$$\therefore \sin\left\{\cos^{-1}(\frac{\mathrm{y}}{2\mathrm{V}_\mathrm{m}\cos\delta}) - \sin^{-1}(\frac{\mathrm{x}}{\mathrm{I}_{\mathrm{m}1}})\right\} = \sin\left(\varphi + \frac{\delta}{2}\right)$$

$$\therefore \left(\frac{\sqrt{(2\mathrm{V}_\mathrm{m}\cos\delta)^2 - y^2}\sqrt{{\mathrm{I}_{\mathrm{m}1}}^2 - x^2} - xy}{2\mathrm{V}_\mathrm{m}\mathrm{I}_{\mathrm{m}1}\cos\delta}\right) = \sin\left(\varphi + \frac{\delta}{2}\right)$$

$$\therefore \sqrt{(2\mathrm{V}_\mathrm{m}\cos\delta)^2 - y^2}\sqrt{{\mathrm{I}_{\mathrm{m}1}}^2 - x^2} - xy = 2\mathrm{V}_\mathrm{m}\mathrm{I}_{\mathrm{m}1}\cos\delta\ \sin\left(\varphi + \frac{\delta}{2}\right)$$

$$\therefore \sqrt{(2\mathrm{V_m}\cos\delta)^2 - y^2}\sqrt{\mathrm{I_{m1}}^2 - x^2} = 2\mathrm{V_m}\mathrm{I_{m1}}\cos\delta\ \sin\left(\varphi + \frac{\delta}{2}\right) + xy$$

Squaring the both sides, we get:

$$\therefore \{(2\mathrm{V_m}\cos\delta)^2 - y^2\}\left\{\mathrm{I_{m1}}^2 - x^2\right\} = \left\{2\mathrm{V_m}\mathrm{I_{m1}}\cos\delta\ \sin\left(\varphi + \frac{\delta}{2}\right) + xy\right\}^2$$

$$\therefore (2\mathrm{V_m}\cos\delta)^2\mathrm{I_{m1}}^2 - (2\mathrm{V_m}\cos\delta)^2 x^2 - \mathrm{I_{m1}}^2 y^2 + x^2y^2 =$$
$$\left\{2\mathrm{V_m}\mathrm{I_{m1}}\cos\delta\ \sin\left(\varphi + \frac{\delta}{2}\right)\right\}^2 + \left\{4\mathrm{V_m}\mathrm{I_{m1}}\cos\delta\ \sin\left(\varphi + \frac{\delta}{2}\right)xy\right\} +$$
$$x^2y^2$$

$$\therefore \{2\mathrm{V_m}\cos\delta\}^2\mathrm{x}^2 + \left\{4\mathrm{V_m}\mathrm{I_{m1}}\cos\delta\ \sin\left(\varphi + \frac{\delta}{2}\right)\right\}\mathrm{xy} + \mathrm{I_{m1}}^2\mathrm{y}^2 +$$
$$\left\{2\mathrm{V_m}\mathrm{I_{m1}}\cos\delta\ \sin\left(\varphi + \frac{\delta}{2}\right)\right\}^2 - (2\mathrm{V_m}\cos\delta\,\mathrm{I_{m1}})^2 = 0 \tag{3.3}$$

Equation (3.3) can be written as:

$$\mathrm{Ax}^2 + \mathrm{Bxy} + \mathrm{Cy}^2 + \mathrm{D} = 0 \tag{3.4}$$

Where:

$$\mathrm{A}=\{2\mathrm{V_m}\cos\delta\}^2$$

$$\mathrm{B}=4\mathrm{V_m}\mathrm{I_{m1}}\cos\delta\ \sin\left(\varphi + \frac{\delta}{2}\right)$$

$$\mathrm{C}=\mathrm{I_{m1}}^2$$

$$D=\left\{2V_m I_{m1}\cos\delta\ \sin\left(\varphi+\frac{\delta}{2}\right)\right\}^2-(2V_m\cos\delta\, I_{m1})^2$$

The quadratic (3.18) represents by:

1. An ellipse if $B^2-4AC<0$
2. A parabola if $B^2-4AC=0$
3. A hyperbola if $B^2-4AC>0$

From equation (3.3), we get:

$$B^2-4AC=16{V_m}^2{I_{m1}}^2(\cos\delta)^2\left(\sin\left(\varphi+\frac{\delta}{2}\right)\right)^2-16{V_m}^2{I_{m1}}^2(\cos\delta)^2$$

$$\therefore B^2-4AC=16{V_m}^2{I_{m1}}^2(\cos\delta)^2\left\{\left(\sin\left(\varphi+\frac{\delta}{2}\right)\right)^2-1\right\}$$

$$\therefore B^2-4AC=16{V_m}^2{I_{m1}}^2(\cos\delta)^2\left\{-\left(\cos\left(\varphi+\frac{\delta}{2}\right)\right)^2\right\}$$

$$\therefore B^2-4AC=-16{V_m}^2{I_{m1}}^2(\cos\delta)^2\left(\cos\left(\varphi+\frac{\delta}{2}\right)\right)^2 \qquad (3.5)$$

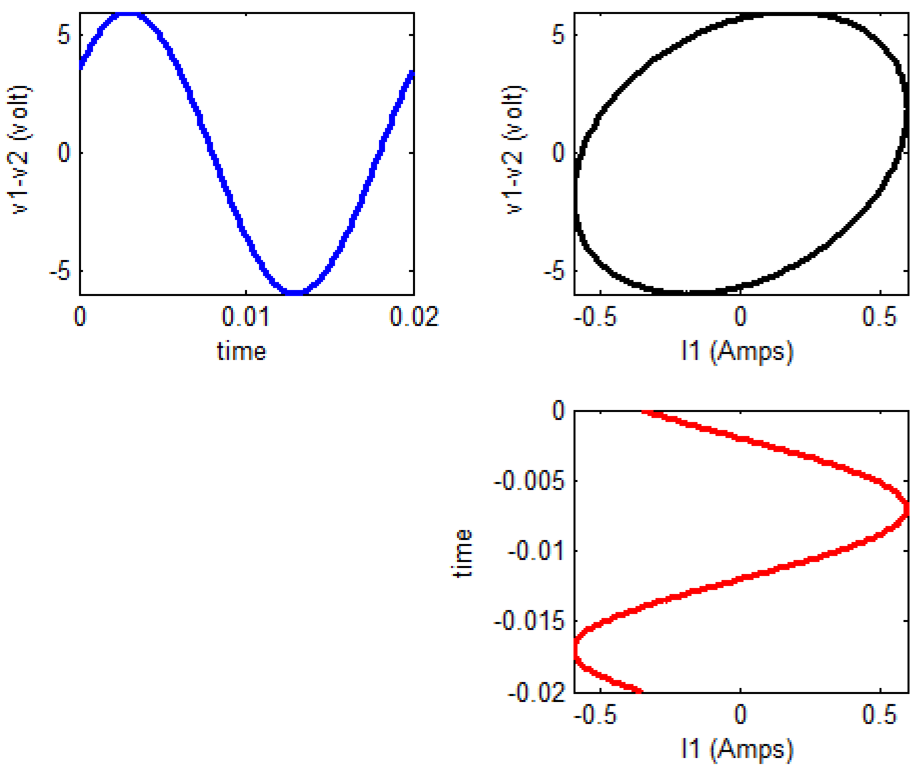

Figure 3.2 Graphical illustration of V-I relationship

Equation 3.5 is always a negative term regardless of the values of $I_{m1}, V_m,\ \delta,$ and, φ. Hence, the Cartesian relationship between ΔV and I_{in} represents an Ellipse. The graphical illustration of the proposed technique is shown in Figure 3.2, where the instantaneous values of ΔV and I_{in} are measured at a particular time to calculate the corresponding point on the (ΔV- I_{in}) locus. The graph in Figure 3.2 is drawn with some assumptions such as (0.8 lagging power factor, the power angle δ can be neglected because the phase shift between V_1 and V_2 is normally small, and the angle Φ between i_1 and V_2 is almost equal to the load impedance phase angle because the phase shift between i_1 and i_2 is negligible).

3.3. Undertaken transformer model

The purpose of the transformer modeling for this study is to analyze the principal changes in (ΔV -I_{in}) locus diagram, which are caused by transformer internal factors. The undertaken transformer for this study is 3 MVA, 33/11 KV, three phase, ONAN, Dy11 power transformer. The adopted model [34] separates the winding into identical sections that simulate individual winding discs. The number of sections is a compromise between closeness to the real transformer and limitations of capability of the program to perform the calculations. An R, L, C equivalent network circuit simulates the transformer winding. Each section of the circuit consists of a ground or shunt capacitance (C_g), series capacitance (C_s), series inductance (L) and resistance (R). The number of sections used in this model is 88, which simulate the number of transformer discs. The series inductance represents the winding lead inductance, the parallel ground capacitance represents the capacitance between the discs and ground, the series capacitance represents the turn-to-turn or disc-to-disc capacitance and the series resistance represents the winding resistance. Figure 3.3 shows the basic model.

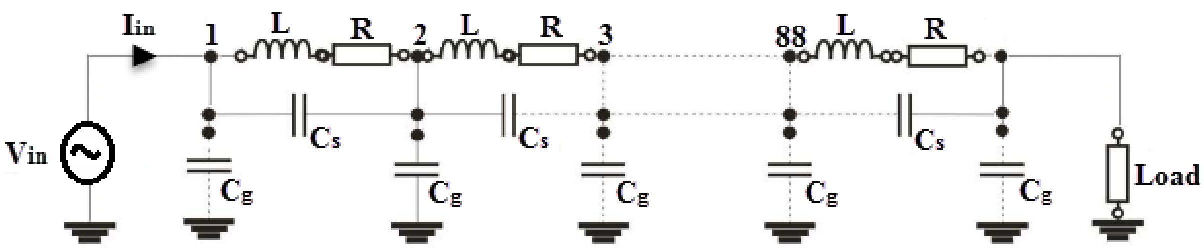

Figure 3.3 Equivalent circuit of a single transformer winding.

The transformer model equivalent circuit shown in Figure 3.3 has been used in this work; the delta-connected disc winding of the HV sides of the transformer has been represented by a network with lumped parameters. The model consists of sequentially arranged 88 discs from line end to earth end of high voltage winding. The model parameters used were based on those used in reference [1]. They were as follows:

R - Resistance per disc	: 0.151 Ω
L - Total inductance per disc	: 0.324 mH
C_s - Series capacitance per disc	: 1.04 nF
C_{sh} - Ground capacitance per disc	: 22.13 pF
S - Total number of sections	: 88

These parameters have been calculated from the practical design data of a 3 MVA, 33/11 kV, three-phase, 50 Hz, ONAN, Dy11 power transformer [34].

3.4. Simulation structure

An integrated model utilizing PSIM Software and MATLAB program was used for simulate the transformer model shown in Figure 3.3. The entire simulation process involved three main stages sequentially run as following:

- Transformer model construction.
- Running Simulations.
- Data file generation.

Figure 3.4 shows the detailed steps for the developed simulation process. The program requires the user to construct the transformer model and input the following data:

- Amplitude of signal.
- Inter turn resistance.
- Inter turn inductance.
- Inter turn capacitance.
- Capacitance to ground.
- Frequency.
- The load impedance.
- Recorded time.
- Time step.

In the proposed model, a 50-Hz ac voltage source of low amplitude is utilized and the instantaneous values of ΔV, I_{in} are recorded at a particular time 0.02 sec. and time step of 10 μsec. The (ΔV- I_{in}) locus diagram of the transformer model under test can be constructed for healthy condition at load impedance (8+j6) Ω. The locus diagram analysis and discrimination will be conducted using MATLAB program and not in the PSIM program. So, we need two sets of data so that we can construct a transformer locus diagram as (ΔV - time) and (I_{in} - time).

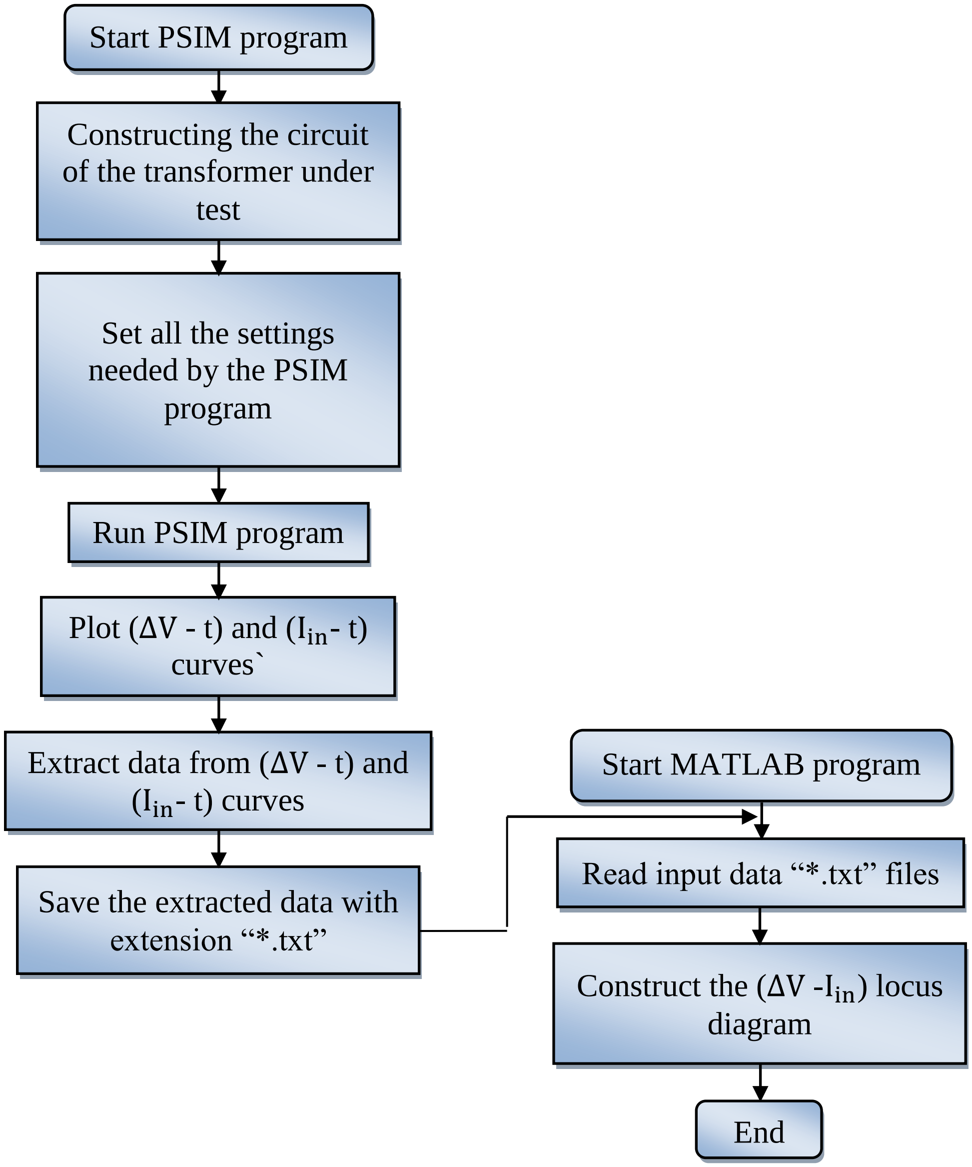

Figure 3.4 Algorithm for developed simulation

3.5. Simulation result

3.5.1. Healthy condition

In this study, the (ΔV- I_{in}) locus diagram of the transformer model under test can be constructed for healthy condition. This locus diagram of a healthy transformer can be shown in Figure 3.5 and is considered as a reference or fingerprint of this transformer.

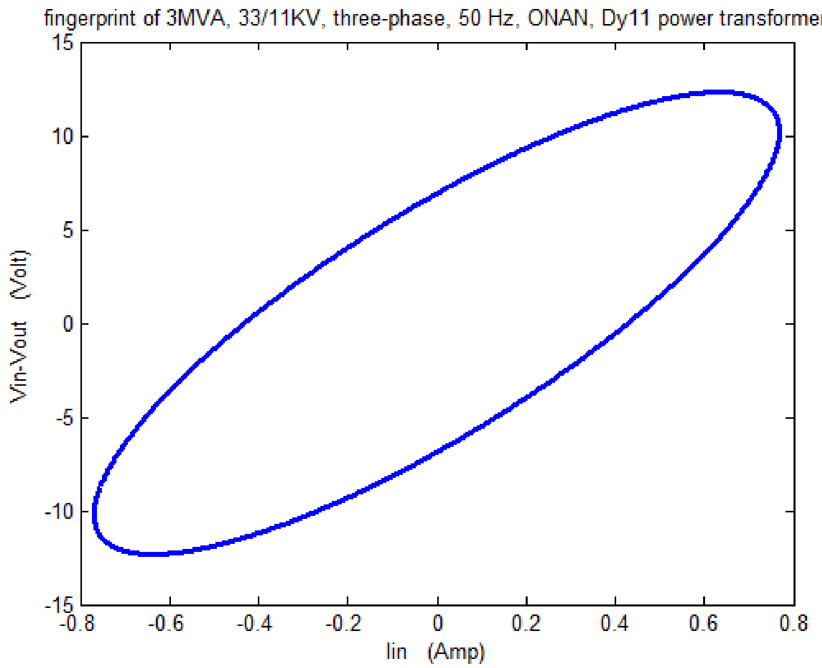

Figure 3.5. Locus diagram of 3MVA, 33/11KV transformer power in healthy condition

3.5.2. Fault conditions

During impulse testing of power transformer, insulation failure/ faults may occur anywhere along the entire length of the transformer winding. The important winding faults, tested via (ΔV- I_{in}) locus analysis, are as follows:

- Partial Discharge (PDF).
- Inter disk fault (IDF).
- Series short circuit (SEF).
- Shunt short circuit (SHF).
- Axial Displacement (ADF).

These faults have been simulated and each faulty locus is compared with the healthy locus (fingerprint) of the proposed transformer.

3.5.2.1. **PDF within transformer winding**

Partial discharges can cause incipient insulation faults, if allowed to develop over time, may lead the insulation to a total breakdown and result in catastrophic failure of power transformers. As an important entity of power plant, loss of a power transformer in operation can lead to economic penalties due to loss of power supply and the capital expenditure for replacement. PD monitoring therefore forms an important part of online condition monitoring and is used as a diagnostic tool for quality of insulation. If during the monitoring process an excessive amount of discharge activity has been detected, the location of discharge needs to be sought in aid of making the decision of either taking the transformer out of service for further investigation or keeping it in operation with increased monitoring [35].

In this work the (ΔV- I_{in}) locus is used for monitoring process of PD. The PD can be simulated by injecting current pulse of shape equivalent to practical PD pulses into probable positions of the windings.

The PD pulse can be approached as different equivalent pulses; such as Gaussian pulse [36] and double exponential [37]. The Gaussian pulse is defined as the following equation:

$$i(t) = I_{max}\left(e^{\frac{-t^2}{2\sigma^2}}\right) \tag{3.6}$$

Where, I_{max} is the magnitude of the peak current in (amperes), t is the time in (seconds), and σ Denotes the pulse width which is chosen to fit the pulse shape with measured pulses and measured at half of the maximum value.

While the double exponential pulse equation can be written as:

$$i(t) = I_{max}[(1 + \alpha t)e^{-\alpha t} - (1 + \beta t)e^{-\beta t}] \tag{3.7}$$

Where, I_{max} is the magnitude of the peak current in (amperes), t is the time in (seconds), and α, β are the time coefficients (reciprocal seconds).

The graphs of Gaussian and double exponential pulses are shown in Figures 3.6 and 3.7 using equations 3.6 and 3.7 respectively.

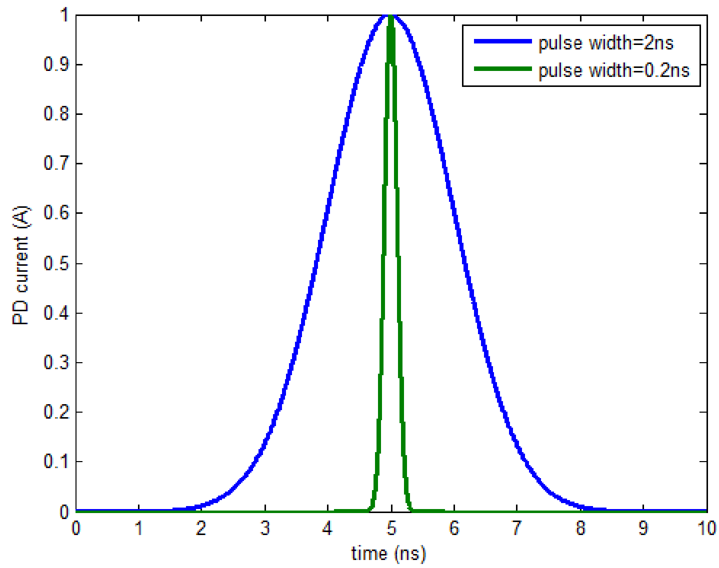

Figure 3.6. PD pulse waveforms using Gaussian pulses of similar current magnitude value but different pulse width

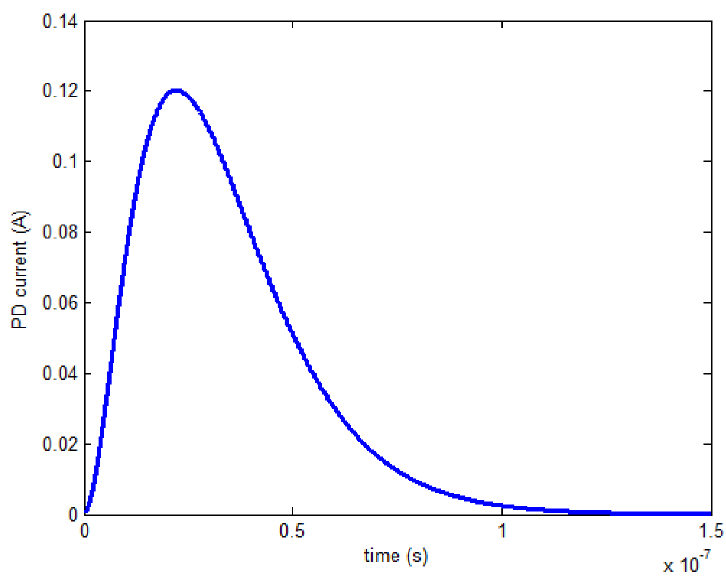

Figure 3.7. PD pulse waveforms using the double exponential pulse equation where

$$(\alpha = 10^8\ sec^{-1}, \beta = 8 * 10^7 sec^{-1})$$

In the proposed model under study, The PD occurrence can be simulated as a current pulse injected into the network nodes 1, 2, 3… N+1 as shown in Figure 3.3.

The PD current pulse is simulated by a Gaussian pulse of 1V peak, pulse width 5 μs as shown in Figure 3.6. Figure 3.8 shows the (Δv -I_{in}) locus for injecting PD pulse for line-end numbers 44 and 48 compared to the healthy locus.

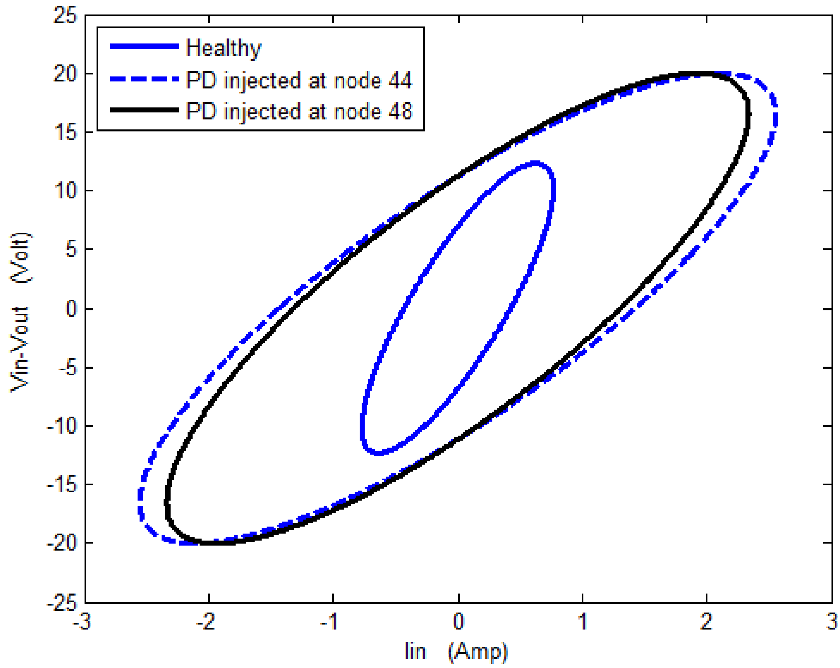

Figure 3.8. The (ΔV -I_{in}) locus for injecting PD pulse at nodes 44 and 48 compared to the healthy locus.

Figure 3.8 shows that PDF will increase the area of the faulty locus compared with the healthy one. Increasing the number of faulty disks will further decrease the locus area and the major axis is rotating in anti-clockwise direction until aligning with the healthy major axis.

3.5.2.2. IDF within transformer winding

One of the most common faults of power transformers is the inter disc fault or (Turn to turn short circuit), as in practice, around 80% of transformer breakdowns are attributed to its occurrence [38]. This fault can be simulated by short circuiting series resistors. In the proposed model under study, during IDF simulation, the series resistors of different number of disks have been short circuited to find their effect on the (ΔV- I_{in}) locus. Figure 3.9 shows the locus for 20 and 60 faulty disks compared to the locus in healthy condition. As the number of faulty disks increases, the locus rotates clockwise and its area increases as illustrated in Figure 3.9.

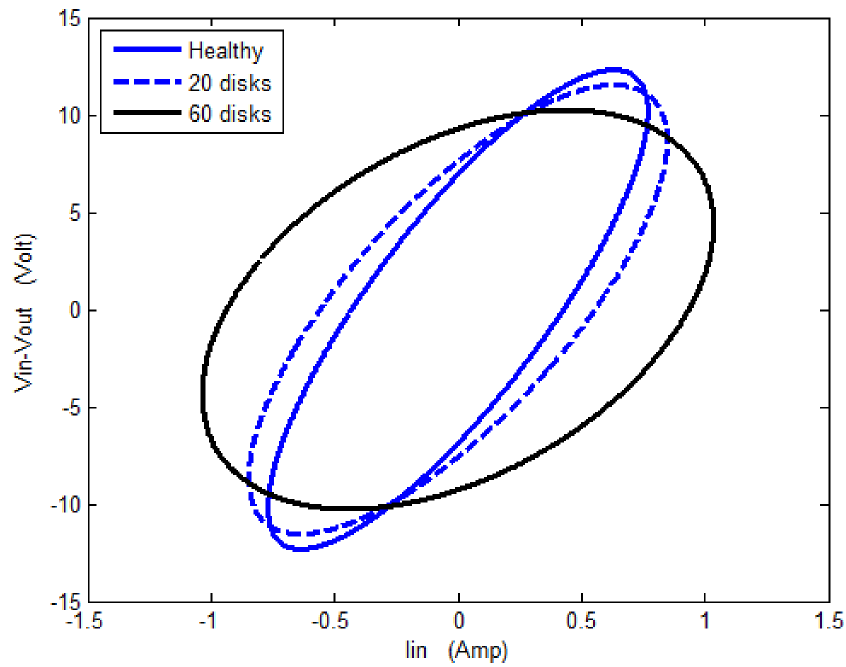

Figure 3.9 Effect of IDF on the (ΔV- I_{in}) locus

3.5.2.3. SEF within transformer winding

Series fault implies insulation failure between the discs. In the proposed model, during SEF simulation, the faulted disc has been short-circuited to find its effect on the (ΔV- I_{in}) locus as shown in Figure 3.10. Figure 3.11 shows the locus for 20 and 80 faulty disks compared to the locus in healthy condition.

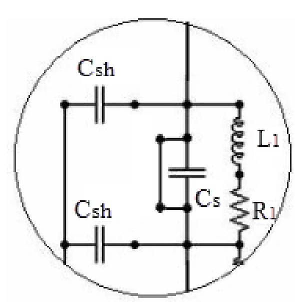

Figure 3.10 Series fault at disc one

It can be observed from Figure 3.11 that as the number of faulty disks increase, the locus rotates in the clockwise direction and its entire area decreases.

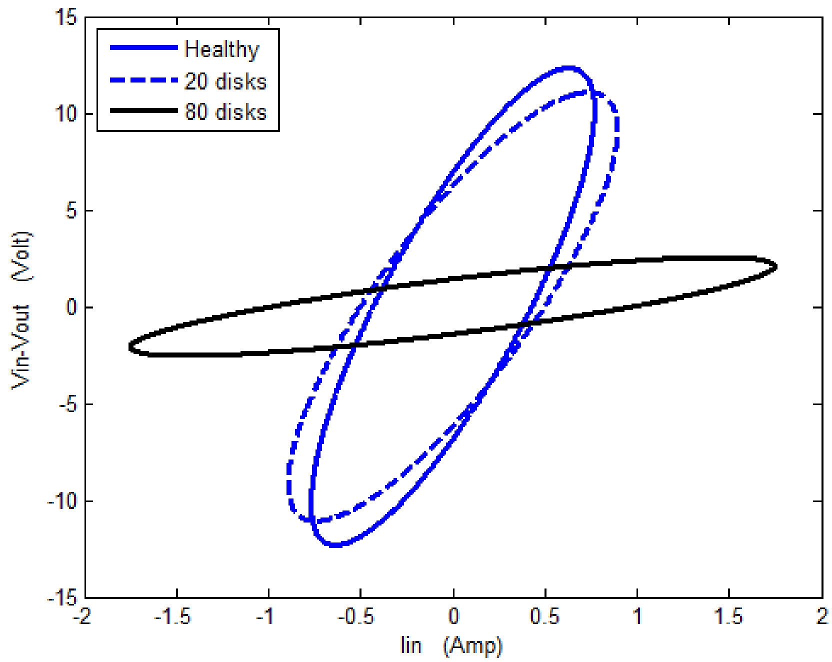

Figure 3.11 Effect of SEF on the (ΔV- I_{in}) locus

3.5.2.4. SHF within transformer winding

Insulation damage, ground shield damage, abrasion, high moisture content in the winding, hotspot and aging insulation, (which reduces its dielectric strength, therefore reducing the resistance to ground) are the main reasons for leakage fault or disc to ground fault inside a transformer [39].

So, shunt fault represents insulation failure between the winding and earthed components, such as tank, core, etc. In the proposed model, this type of fault can be simulated by connected the faulty disc to ground as shown in Figure 3.12. Figure 3.13 shows the locus for 20 and 60 faulty disks compared to the locus in healthy condition.

It can be observed from Figure 3.13 that as the number of faulty disks increase, the locus rotates in the clockwise direction and its entire area increases.

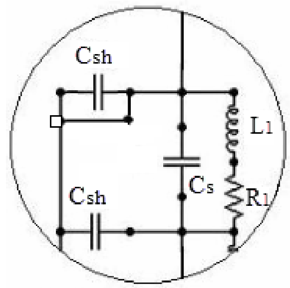

Figure 3.12 Shunt fault at disk one

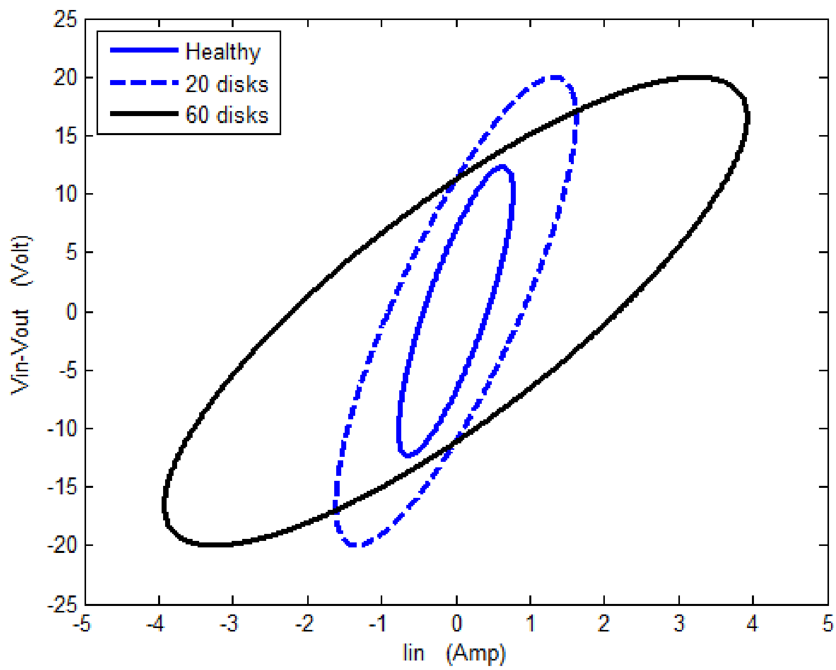

Figure 3.13 Effect of SHF on the (ΔV- I_{in}) locus

3.5.2.5. **ADF within transformer winding**

In the case of short circuit currents, ADF occurs due to the magnetic imbalance between low and high voltage windings. The axial displacement between the magnetic centers of the windings will result in unbalanced magnetic force components in each half of the winding which leads to a change in its relative position. Leaving this fault without monitoring can cause winding collapse or failure of the end-supporting structure due to its progressive nature [6].

Generally, this type of fault can be simulated by changing the mutual and self-inductances of particular disks. The change in capacitance can be neglected [38].

In the proposed model under study, The ADF is simulated by decrease the inductance by 30% of its value. The effect of axial displacement of 60 and 88 disks on the (ΔV- I_{in}) locus compared to the locus in healthy condition is illustrated in Figure 3.14. Axial displacement will decrease the area of the faulty locus compared with the healthy one as Increasing the number of faulty disks will further decrease the locus area but with a very slight decrease in the locus major axis and thus can be neglected. So, approximately no rotation in the locus major axis.

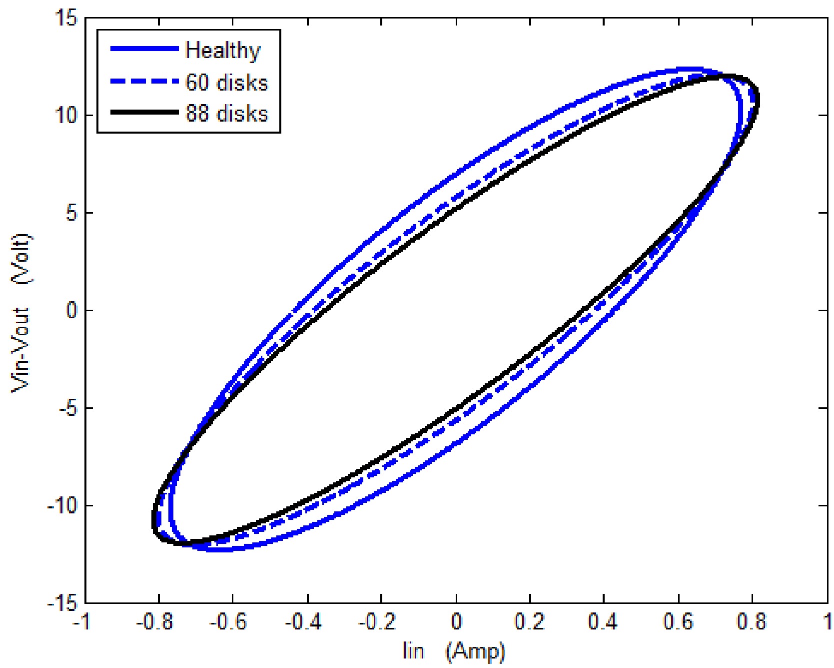

Figure 3.14 Effect of ADF on the (ΔV- I_{in}) locus

CHAPTER FOUR

4. FAULT DISCRIMINATION

4.1. Visual discrimination

Discrimination between different types of faults can be visibly observed from the (ΔV - I_{in}) locus area and major axis rotation. To show this, different types of faults discussed before are simulated on 40 disks of the transformer model, and the (ΔV -I_{in}) loci for all of them with respect to the healthy locus are compared as shown in Figure 4.1.

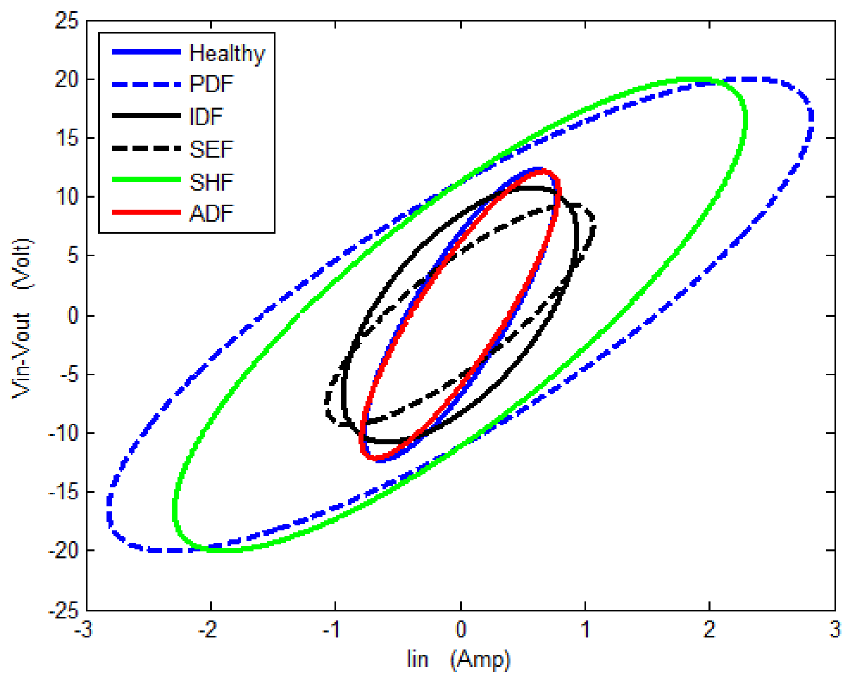

Figure 4.1 Comparison of the effect of each fault on the (ΔV- I_{in}) locus (40 disks)

Figure 4.1 shows that the locus area is increasing in all faulty cases with respect to the area of the healthy locus except in cases of axial displacement and series short circuit where the area is decreased. The locus major axis in case of axial displacement is aligning with the healthy major axis but in other cases the major axis will rotate in the clockwise or anti clockwise directions (according to the type of the applied fault) in the case of the number of faulty disks increases.

Table 4.1 summarizes the effect of studied faults on the locus area and locus major axis rotation in relation to the healthy locus for visual discrimination.

Table 4.1 Effect of faults on locus area and axis rotation

Simulation No.	**Fault type**	**indication**	
		Area	**Rotation**
Simulation 1	PDF	Significant increase	Very large
Simulation 2	IDF	increase	large
Simulation 3	SEF	decrease	Large
Simulation 4	SHF	increase	large
Simulation 5	ADF	decrease	none

4.2. Fault discrimination using traditional techniques

This section reviews two methods used for fault discrimination within transformer windings based on image processing. These methods tested by applying the most types of fault winging that produced within transformer winding such as turn to turn short circuit, axial displacement, disk to ground fault and buckling stress of inner winding.

4.2.1. Image pixels discrimination

This method has been introduced by [38], and by using that a rough approximation of the contour length can be measured by counting the number of pixels along the contour. A MATLAB code has been introduced to measure the number of pixels for healthy and faulty loci [40]. Same axes scales were used in plotting all loci. Results in [38] shows that the turn to turn short circuit fault has significant increase in number of pixels as the number of faulty disks increases compared to the healthy case.

4.2.2. Mean square error

This method has concentrated on determining the root mean square (RMS) error of the locus diagram. A MATLAB code has been developed to measure the RMS error of the faulty loci compared to the healthy locus. The images are converted into a two dimensional array with values representing pixel colors. The faulty image array and healthy image array are then used to calculate the RMS error.

Results in [38] shows that the RMS error for all types of faults increases as the number of faulty disks increases. Results also shows that the turn to turn short circuit has the largest RMS error while the disk to ground fault has the minimum RMS error.

The main problem in these two techniques that the image may contain noise in the case of fault occurrence. Thus, this work undertakes feature extraction from the faulty loci compared to the healthy locus to improve the discrimination process and this is described in the following section.

4.3. Feature extraction

After simulation of insulation failures; as has been shown in the mathematical proof and simulation results before, the (ΔV - I_{in}) locus is always representing an ellipse. The next goal of the present thesis is identification and location of fault characteristics, i.e. type and location of failures. So, some unique features of the ellipse can be used to compare different loci and to identify the type of fault within the power transformer. Some of significant features are extracted from each of 440 loci. These features include ellipse centroid, the major axis length (a), the minor axis length (b), the angle between the major axis, and the horizontal axis (θ) as shown in Figure 4.2, and hence calculate ellipse focus (f), eccentricity (e), flattering (g), and area ($A_{ellipse}$), and circumference ($C_{\boldsymbol{ellipse}}$).

Basically, the ellipse which depicts in Figure 4.3 is constructed from two waves (E_x, Z) and (E_y, Z) illustrated in Figure 4.2.

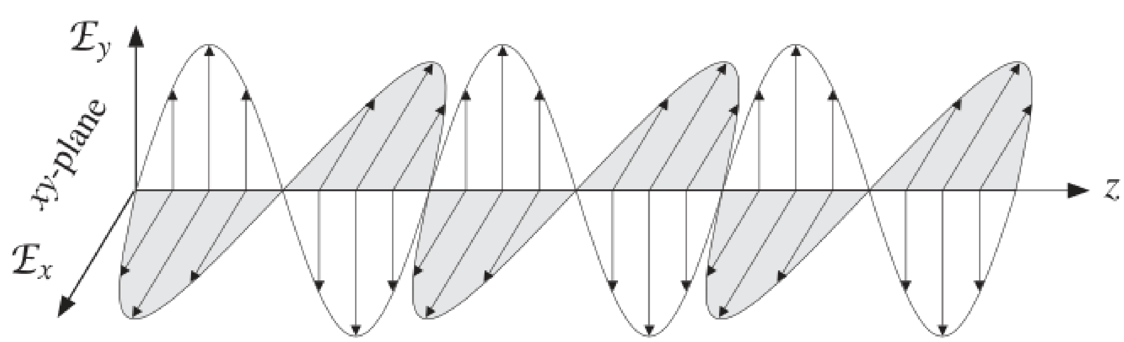

Figure 4.2 Uniform plan wave.

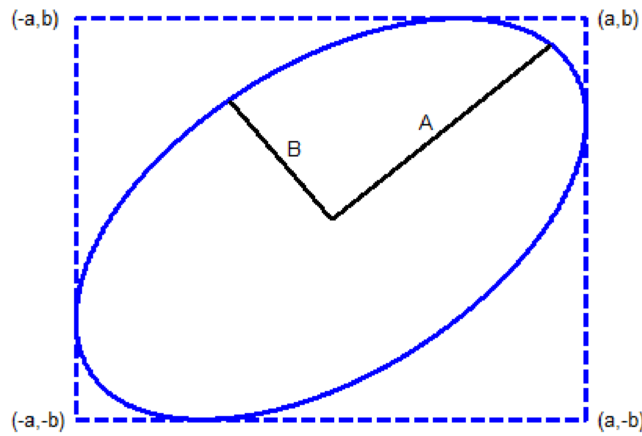

Figure 4.3 General ellipse

Two options are provided for the calculating of the ellipse axes lengths A', and B'. The first is presented by [41] and it is present a MATLAB function to calculate the ellipse axes A', and B' by using the magnitude of the two waves (A, B) and the phase shift between them (φ). This function carried out by using the following equations:

$$\mathrm{A} = \sqrt{\frac{1}{2}(\mathrm{a}^2 + \mathrm{b}^2) + \frac{\mathrm{s}}{2}\sqrt{(\mathrm{a}^2 - \mathrm{b}^2)^2 + 4\mathrm{a}^2\mathrm{b}^2\cos^2\varphi}} \quad (4.1)$$

$$\mathrm{B} = \sqrt{\frac{1}{2}(\mathrm{a}^2 + \mathrm{b}^2) - \frac{\mathrm{s}}{2}\sqrt{(\mathrm{a}^2 - \mathrm{b}^2)^2 + 4\mathrm{a}^2\mathrm{b}^2\cos^2\varphi}} \quad (4.2)$$

Where s=sign (a-b).

The second option is development a MATLAB code to also calculate the ellipse axes a, and b by using the ellipse (x-y) data. The two options have been tested on a different numbers of ellipse and table 4.2 gives the output ellipse axes.as follows:

Ellipse 1: $E_x(t) = 4\cos(\omega t + \pi), E_y(t) = 3\cos(\omega t)$

Ellipse 2: $E_x(t) = 3\cos(\omega t + \frac{\pi}{3}), E_y(t) = 3\cos(\omega t)$

Ellipse 3: $E_x(t) = 4\cos(\omega t), E_y(t) = 3\cos(\omega t - \frac{\pi}{4})$

Ellipse 4: $E_x(t) = 4\cos(\omega t + \frac{\pi}{4}), E_y(t) = 3\cos(\omega t - \frac{\pi}{2})$

Table 4.2 Ellipse axes output

Ellipse no.	Method no. 1		Method no. 2	
	A	**B**	**A**	**B**
1	5.0000	0	5	0.001018366018475
2	3.6742	2.1213	3.674234614128865	2.121320426347296
3	4.6560	1.8224	4.619553796225180	1.913303292001840
4	4.6560	1.8224	4.619350467616694	1.913794857248074

In this thesis. It was found that the second option is sufficiently suitable with the type of data of ellipses. The other ellipse features as mentioned before can be calculated from the following relations [42]:

$$\theta = \frac{1}{2}\operatorname{atan}\left\{\frac{2AB}{A^2-B^2}\cos\varphi\right\} \tag{4.3}$$

The first and second ellipse eccentricity e, e' and its relation between them are given by equations 4.4, 4.5, and 4.6 respectively.

$$e = \frac{f}{a} = \frac{\sqrt{A^2-B^2}}{A} \tag{4.4}$$

$$e' = \frac{f}{b} = \frac{\sqrt{A^2-B^2}}{B} \tag{4.5}$$

$$\frac{e}{e'} = \frac{B}{A} \tag{4.6}$$

The ellipse focus (f) and flattering (g) can be calculated from equations 4.7, and 4.8. While the ellipse area and circumference are given by equations 4.9, and 4.10.

$$f = \sqrt{A^2 - B^2} \tag{4.7}$$

$$g = 1 - \frac{B}{A} \tag{4.8}$$

$$A_{\mathrm{ellipse}} = \pi AB \tag{4.9}$$

$$C_{\mathrm{ellipse}} \approx \pi\left\{3(A+B) - \sqrt{10AB + 3(A^2+B^2)}\right\} \tag{4.10}$$

Moreover, to get better fault identification accuracy, three features are also extracted using statistical analysis of the load voltage. These features are given by:

$$V_{L_{\mathrm{av}}} = \frac{1}{2\pi}\int_0^{2\pi} V_{\mathrm{m}} \sin(wt)\ dwt \tag{4.11}$$

$$V_{L_{\mathrm{rms}}} = \sqrt{\frac{1}{2\pi}\int_0^{2\pi} (V_{\mathrm{m}} \sin(wt))^2\ dwt} \tag{4.12}$$

$$V_{L_{\mathrm{abs}}} = \left|\frac{1}{2\pi}\int_0^{2\pi} V_{\mathrm{m}} \sin(wt)\ dwt\right| \tag{4.13}$$

A MATLAB code is developed to extract and calculate all of these features. Table 4.3 represents general ellipse features of healthy condition for the transformer under test.

Table 4.3: General ellipse features for healthy condition.

Ellipse features									
A	**B**	**θ**	**f**	**e**	**e′**	$\frac{e}{e'}$	**g**	$A_{ellipse}$	$C_{ellipse}$
11.79899	3.623187	86.42625	11.22893	0.951685	3.099185	0.307076	0.692924	134.303	51.91633

4.4. Computational discrimination

Locus area and locus angle of rotation can be measured by equations 4.9 and 4.3 respectively. A MATLAB code is developed to measure the locus area and the angle of rotation of the faulty loci compared to the healthy locus. Figures 4.4 and 4.5 shows the effect of faults on locus area and locus angle of rotation.

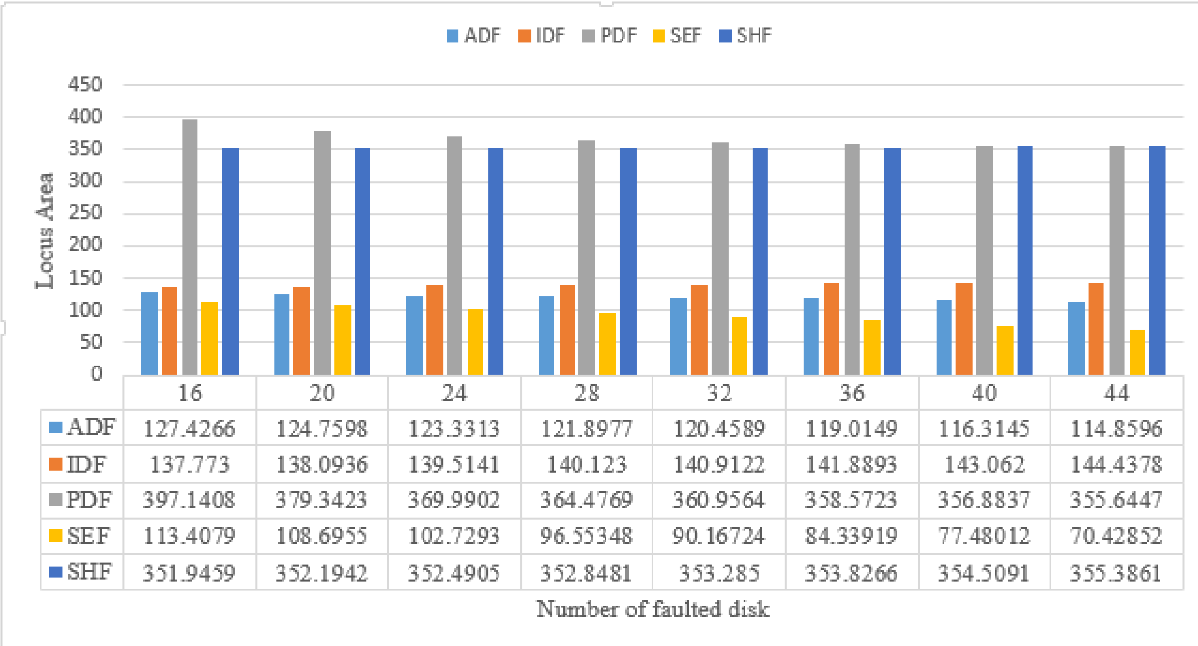

	16	20	24	28	32	36	40	44
ADF	127.4266	124.7598	123.3313	121.8977	120.4589	119.0149	116.3145	114.8596
IDF	137.773	138.0936	139.5141	140.123	140.9122	141.8893	143.062	144.4378
PDF	397.1408	379.3423	369.9902	364.4769	360.9564	358.5723	356.8837	355.6447
SEF	113.4079	108.6955	102.7293	96.55348	90.16724	84.33919	77.48012	70.42852
SHF	351.9459	352.1942	352.4905	352.8481	353.285	353.8266	354.5091	355.3861

Figure 4.4 Effect of faults on locus area

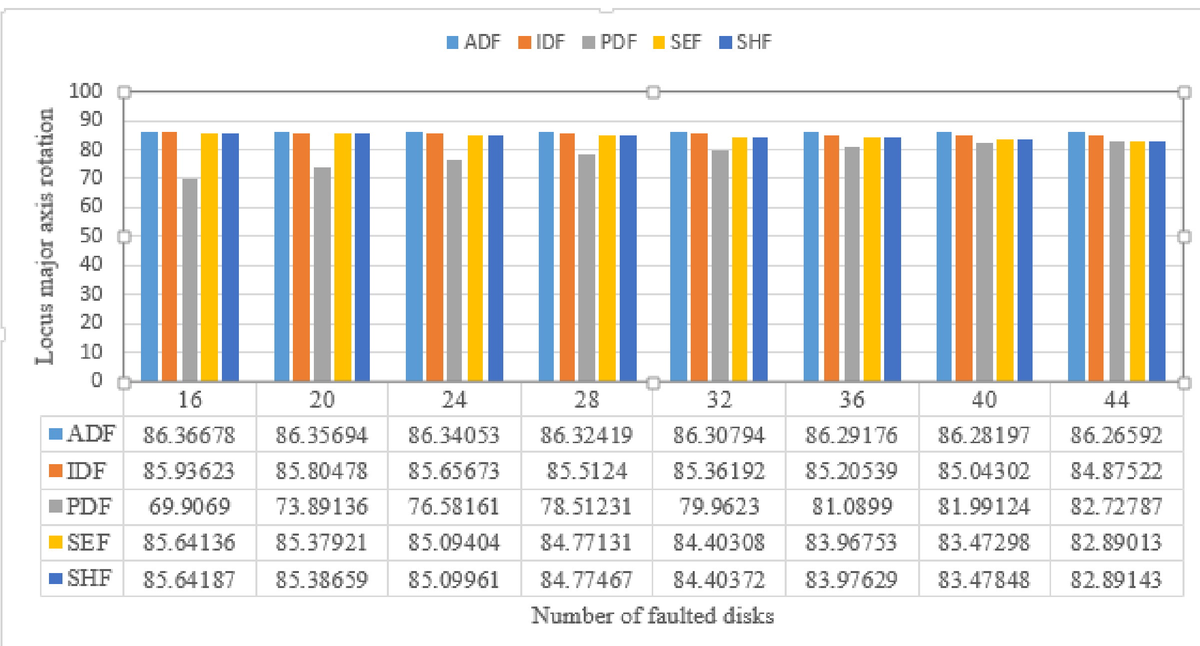

	16	20	24	28	32	36	40	44
ADF	86.36678	86.35694	86.34053	86.32419	86.30794	86.29176	86.28197	86.26592
IDF	85.93623	85.80478	85.65673	85.5124	85.36192	85.20539	85.04302	84.87522
PDF	69.9069	73.89136	76.58161	78.51231	79.9623	81.0899	81.99124	82.72787
SEF	85.64136	85.37921	85.09404	84.77131	84.40308	83.96753	83.47298	82.89013
SHF	85.64187	85.38659	85.09961	84.77467	84.40372	83.97629	83.47848	82.89143

Figure 4.5 Effect of faults on locus angle of rotation

Table 4.4 shows the difference in locus area ($A_{ellipse}$) and the locus major axis rotation (θ) for different types of faults for the whole winding of the transformer under test with respect to the healthy locus for computational discrimination. Unlike the series fault and axial displacement fault, the locus area for the inter disk fault and shunt fault increase as the number of faulty disks increases while the partial discharge fault has a significant increase of locus area as the number of faulty disks increases and this can be shown in Figure 4.4 and table 4.4. Also as can be shown in Figure 4.4 and table 4.4, the locus angle of rotation for the axial displacement fault remains constant as the number of faulty disks increases. While in the case of partial discharge fault, the locus angle of rotation increase so much as the number of faulty disks increases. In the case of the inter turn fault occurrence, the locus angle of rotation increase as the number of faulty disks increases. And this is coherent with the locus displayed in section 4.1.

Table 4.4 Effect of different faults on locus area and axis rotation

Faulty disc	**Axial displacement**		**Inter turn**		**Partial discharge**		**Series fault**		**Shunt fault**	
	$A_{ellipse}$	**θ**	$A_{ellipse}$	**θ**	$A_{ellipse}$	**θ**	$A_{ellipse}$	**θ**	$A_{ellipse}$	**θ**
4	131.5466	86.41504	134.1752	86.31839	1530.998	28.66675	129.3579	86.25782	351.4018	86.26255
8	130.139	86.39844	135.3264	86.19759	566.8361	51.90776	124.2314	86.07269	351.5562	86.07625
12	128.7262	86.3819	136.524	86.07033	437.7482	63.48843	118.9168	85.86827	351.7357	85.87043
16	127.4266	86.36678	137.773	85.93623	397.1408	69.9069	113.4079	85.64136	351.9459	85.64187
20	124.7598	86.35694	138.0936	85.80478	379.3423	73.89136	108.6955	85.37921	352.1942	85.38659
24	123.3313	86.34053	139.5141	85.65673	369.9902	76.58161	102.7293	85.09404	352.4905	85.09961
28	121.8977	86.32419	140.123	85.5124	364.4769	78.51231	96.55348	84.77131	352.8481	84.77467
32	120.4589	86.30794	140.9122	85.36192	360.9564	79.9623	90.16724	84.40308	353.285	84.40372
36	119.0149	86.29176	141.8893	85.20539	358.5723	81.0899	84.33919	83.96753	353.8266	83.97629
40	116.3145	86.28197	143.062	85.04302	356.8837	81.99124	77.48012	83.47298	354.5091	83.47848
44	114.8596	86.26592	144.4378	84.87522	355.6447	82.72787	70.42852	82.89013	355.3861	82.89143
48	113.3995	86.24996	145.1795	84.70262	354.7074	83.34096	63.77555	82.17827	356.5392	82.18895
52	111.9343	86.23411	147.2846	84.54534	353.9813	83.85907	56.34134	81.32846	358.0976	81.33359
56	110.464	86.21837	148.8905	84.38902	353.4094	84.30264	49.24094	80.25398	360.2764	80.26988
60	108.9886	86.20274	150.8593	84.23591	352.9485	84.68661	41.60863	78.90438	363.4543	78.91223
64	106.248	86.19314	153.2117	84.08884	352.5737	85.02222	34.33012	77.1016	368.3506	77.12168
68	104.7615	86.17769	155.3069	83.9513	352.2634	85.31803	26.89909	74.65107	376.471	74.65791
72	103.2699	86.16236	159.5512	83.85686	352.0032	85.58073	20.02041	71.05106	391.4197	71.07068
76	101.7732	86.14718	162.2543	83.7222	351.7835	85.81557	13.70214	65.39216	423.7163	65.42706
80	100.2715	86.13213	166.9466	83.67567	351.2628	86.01913	8.345536	55.55381	515.9915	55.5539
84	97.49592	86.12277	170.7752	83.59042	351.4365	86.21766	4.675599	36.08834	1014.27	36.09104
88	95.98299	86.10795	309.0184	86.55706	351.2997	86.39108	0.006661	5.73E-05	695070.8	5.73E-05

CHAPTER FIVE

5. ARTIFICIAL INTELLIGENCE BASED FAULT IDENTIFICATION

Fault identification and location according to FRA can be performed by experienced engineers. However, the problem is the relations and patterns based FRA, although present, are too complex to humanly discern so that a rule base cannot be built manually. As so far, there is no standard code for FRA interpretation worldwide. To solve this problem, various artificial intelligence techniques have been proposed in the literature. The techniques include expert systems, back propagation artificial neural network (BPANN), radius function network (RBF), propagations neural network (PNN), self-organizing map (SOM) network, and learn vector quantization (LVQ) algorithm [1-6].

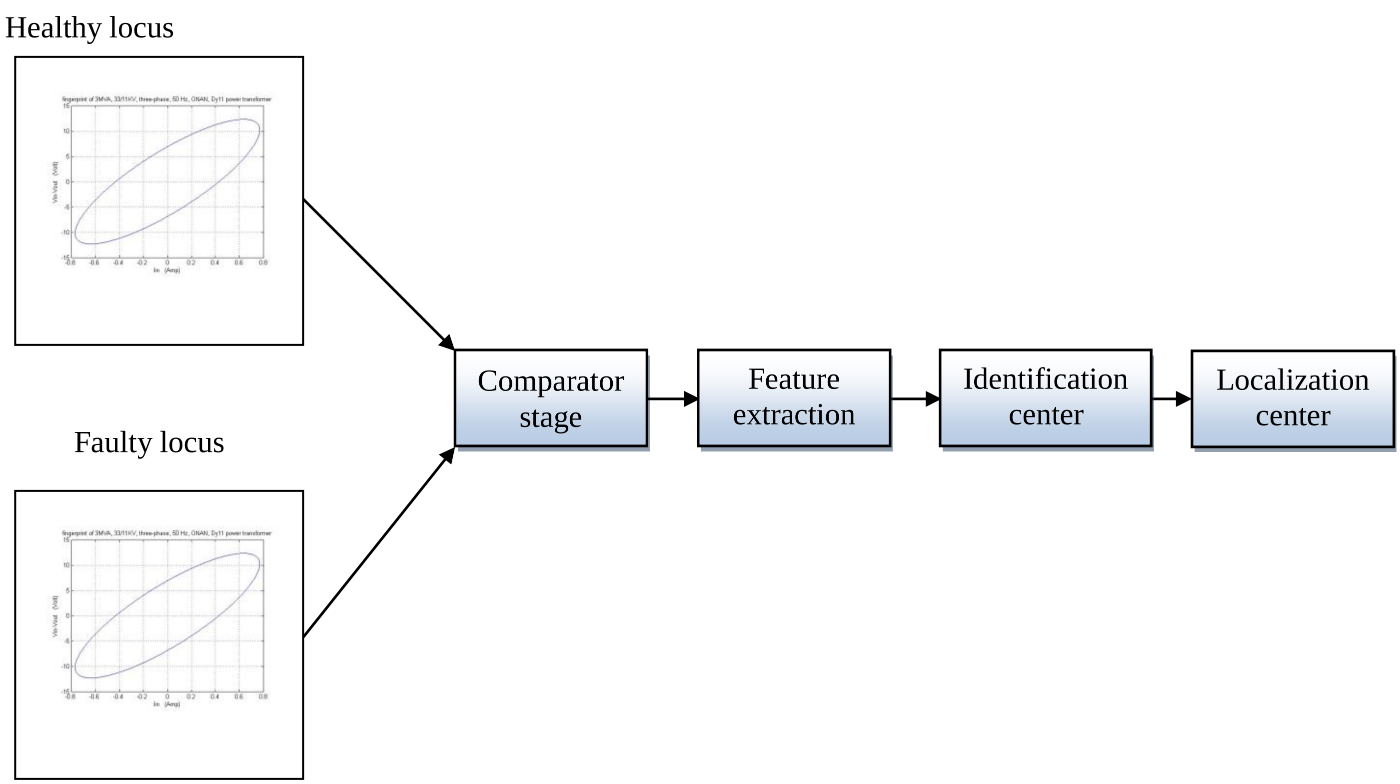

Figure 5.1. Block diagram representation of fault identification and localization scheme

In this thesis, the problem is to assign "unknown" fault patterns to known there classifications and locations. In this approach the identification scheme, as shown in Figure 5.1, will be developed and employed to perform the detection and location tasks of the diagnostic system using two different structures of intelligent techniques which can be summarized as follows:

5.1. Conventional fault classification technique (if-condition based image comparator).

Any mechanical fault within transformer winding will alter the locus in a unique way and, hence, fault detection as well as fault type can be identified. A new classification technique based on measuring and comparing some features of the loci to identify the possible fault type is developed. These features include locus area, and the locus angle of rotation.

As mentioned before, the used FRA technique does not call for any new hardware since it uses the existing metering devices attached with the power transformer and can be implemented online as it is performed at the power frequency. The proposed locus can be plotted every cycle (20 ms based on a 50-Hz network). And compared with the healthy locus using the developed image-processing code to immediately identify any changes, it generates an early warning signal.

To identify the type of fault based on locus area, angle of rotation, the proposed model is divided into twenty two sections, viz. S1, S2… S22. Each fault has been simulated on a different number of discs starting from one section to 22 sections, and these parameters are calculated for each fault. Each section consists of sequentially arranged 4 disks and covers approximately 4.5 % of winding length, i.e., the developed algorithm had localized and identified different five types of insulation failures within ±4.5 % of winding length. This ± 4.5 % of the localization length has been obtained by trial and error method. It was observed that, higher value of fault identification accuracy may be obtained with minimum number of winding section, like, three sections and each covers 33% of winding length [3].

Based on the range of the percentage differences of these parameters for each fault, the MATLAB code is developed to identify and locate fault within the transformer windings.

The logic flow diagram of fault identification using their extracted features is shown in Figure 5.2.

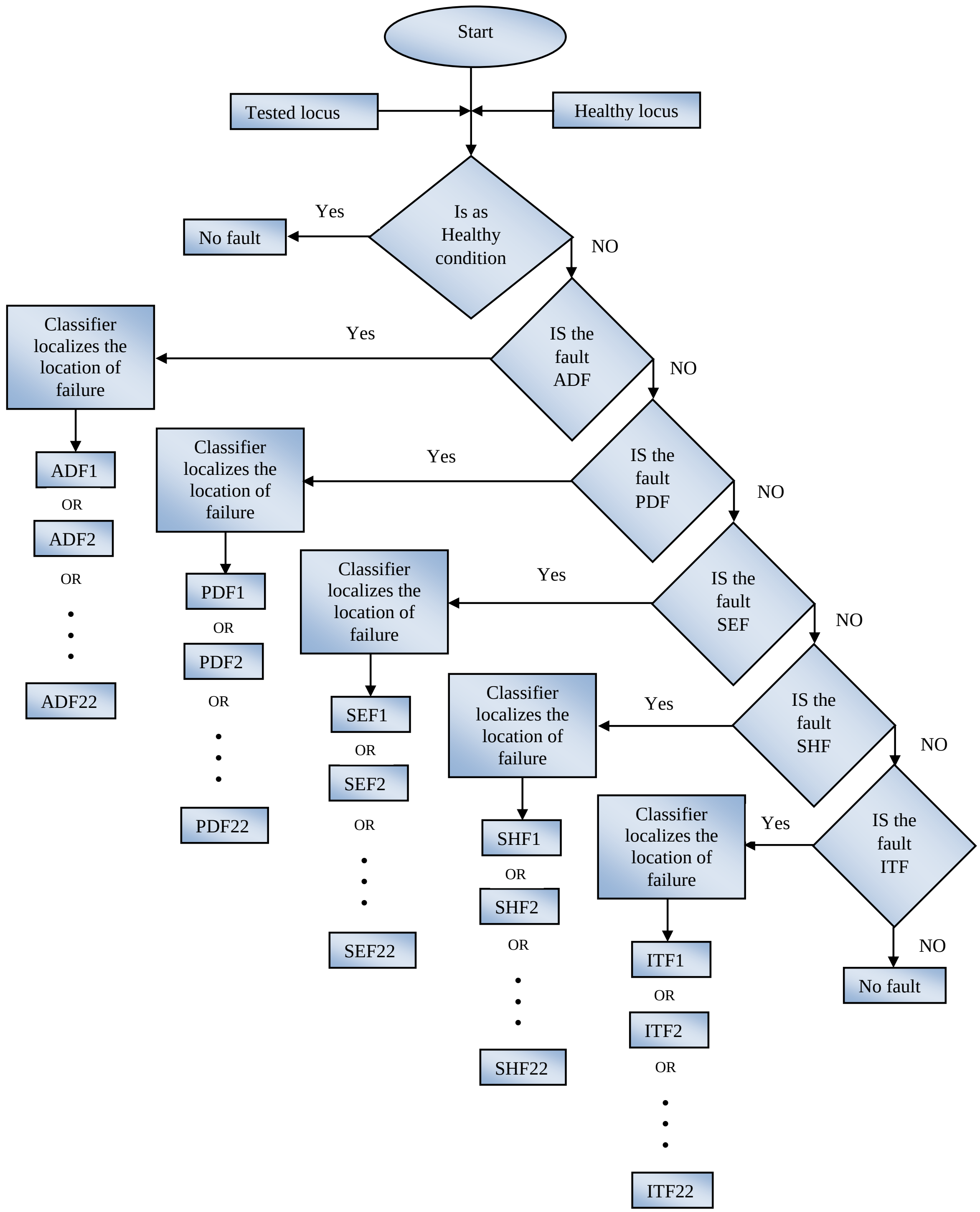

Figure 5.2. Logic flow diagram for identification of fault characteristics

It may be observed that the algorithm work in two levels. In the first level of classifier, the insulation failure is identified as (SEF) or (IDF) or (ADF) or (PDF) or (SHF). Then, the location of insulation failure within 22 sections of the winding is predicted in the level 2 classifier as S1 or S 2 or S3... or S22.

Usage of intelligence techniques is the challenge of this trend to get more accuracy for fault identification. The next section discusses ANNs, the tool that is being explored to develop the advanced diagnostic framework for frequency response fault diagnoses (FRFD).

5.2. Results and discussion

The preconditioning of the input data is the important facet of classification based neural network. The features that has been extracted from the frequency response of a transformer is essentially a series of values corresponding to the state of the winding. As mentioned before, the used FRA technique relies on recording the (ΔV- I_{in}) diagram by using the metering devices that already attached to the transformer. Thus, this technique is conducts on line at the nominal power frequency. The locus diagram can be recorded every 20 ms (cycle). Any type of fault produced inside the transformer winding will affect the locus, hence, the new locus can be used to identify the type of fault. A new LVQ classification technique based on identify the extracted features from the faulty loci to get the type of fault is introduced. The extracted features from ellipse general proportion of various faulted conditions forms thirteen-dimensional data matrix $Xm \times n$ where m is the fault cases and n is the features of each case of fault. These features contain the fault characteristics. In this work, m is 440 case corresponding to five different abnormal conditions at 88 different location within transformer winding. So, the data matrix that used for the identification contains 440 fault classes (rows) and 13 features (columns). The LVQ algorithm is performed to find classes. The fault identification results based on LVQ show that this number of features are sufficient to get a reasonably good accuracy in the identification task.

According to the transformer model under study, an 88 different locations apt to five types of fault conditions along the transformer winding. So, we have five classes. To show this classes, each two features are plotted together for all five classes. Figure 5-3 to 5-14 depicts the first feature (ellipse area) against the residual features.

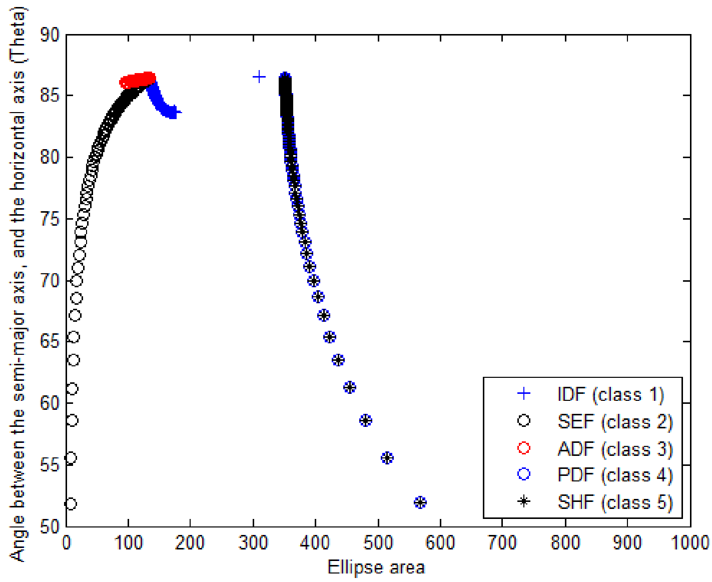

Figure 5-3 the five classes according to two features (area and theta)

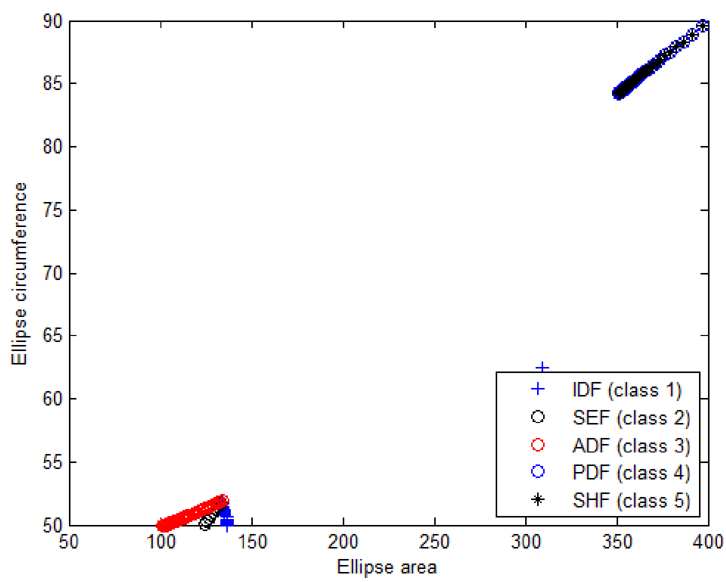

Figure 5-4 the five classes according to two features (area and circumference)

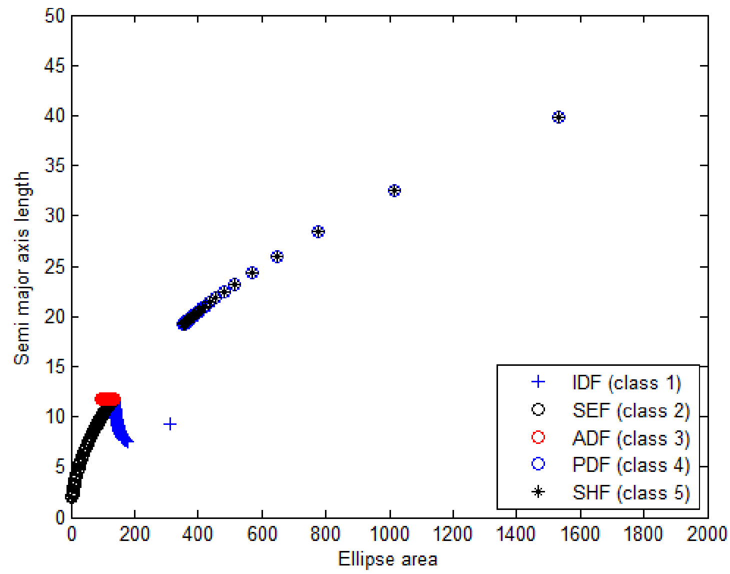

Figure 5-5 the five classes according to two features (area and semi major axis length)

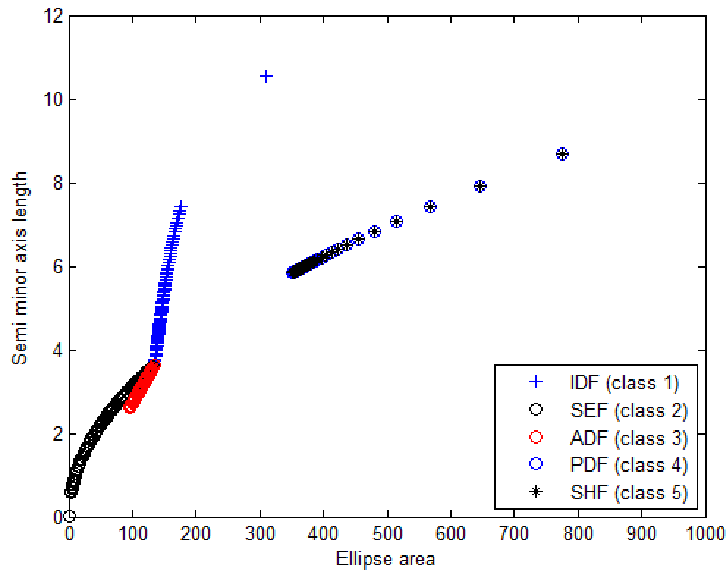

Figure 5-6 the five classes according to two features (area and semi minor axis length)

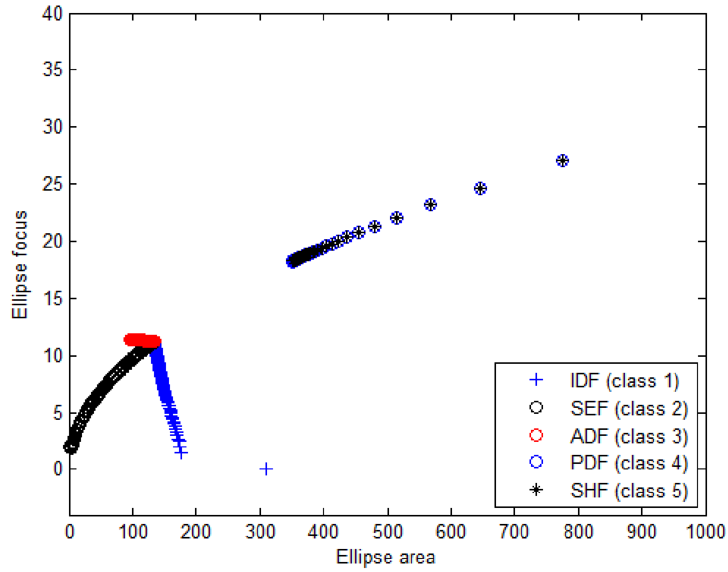

Figure 5-7 the five classes according to two features (area and focus)

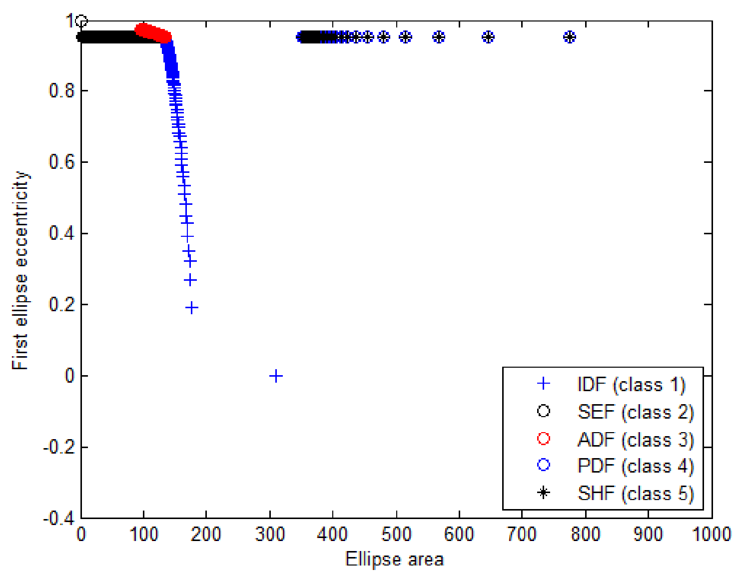

Figure 5-8 the five classes according to two features (area and first eccentricity)

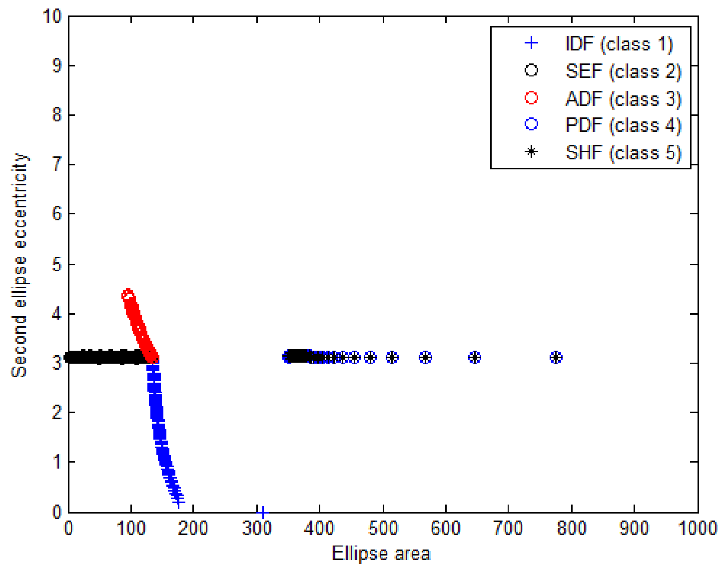

Figure 5-9 the five classes according to two features (area and second eccentricity)

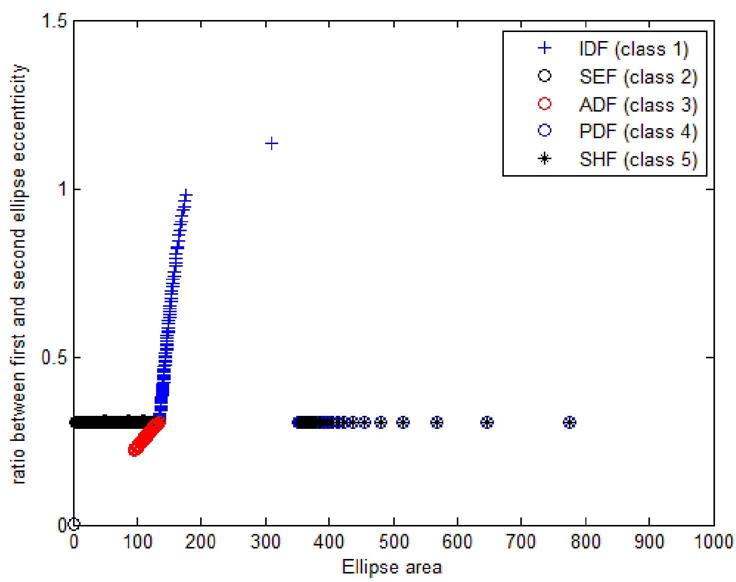

Figure 5-10 the five classes according to two features (area and ratio between eccentricities)

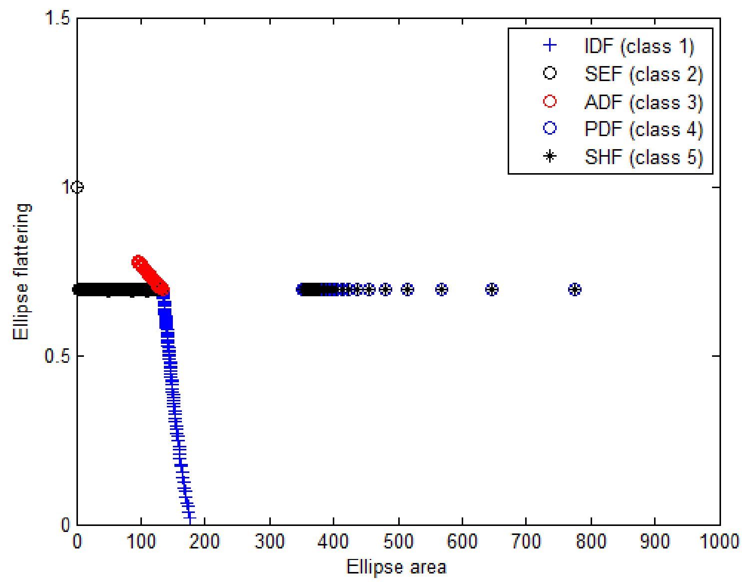

Figure 5-11 the five classes according to two features (area and flattering)

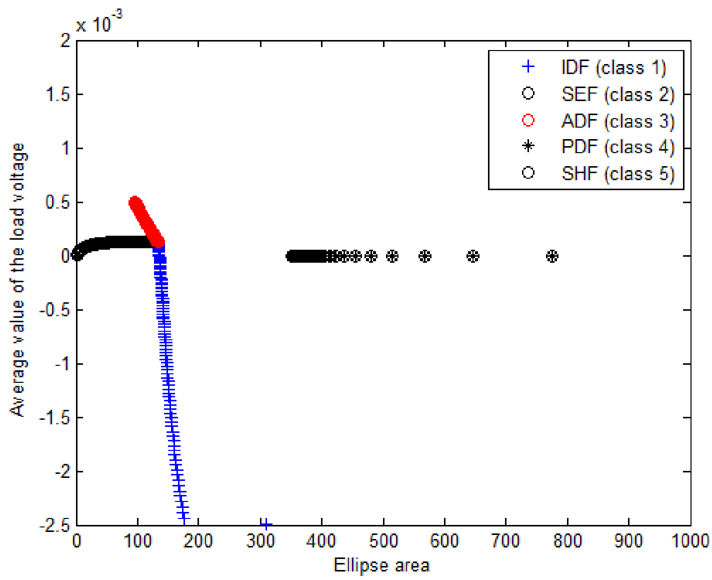

Figure 5-12 the five classes according to two features (area and average value of load voltage)

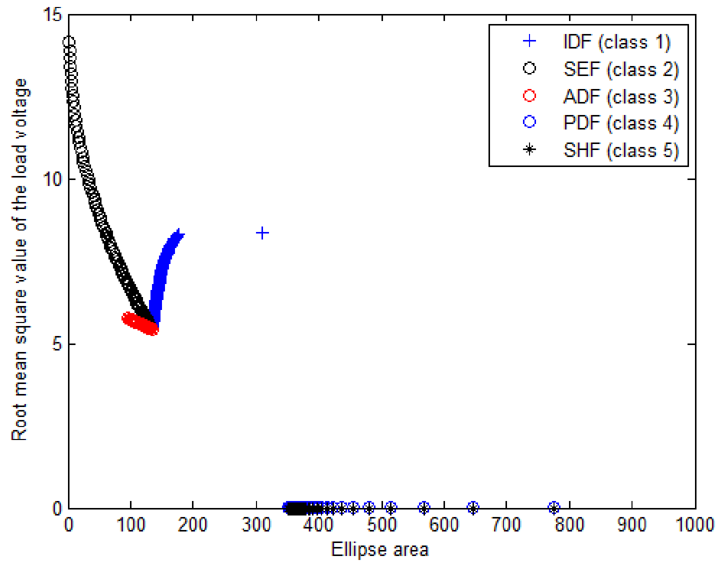

Figure 5-13 the five classes according to two features (area and root mean square value of load voltage)

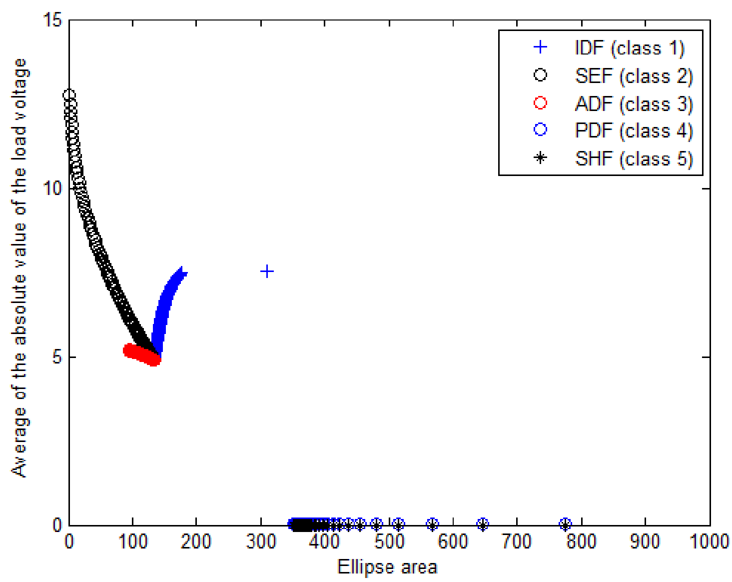

Figure 5-14 the five classes according to two features (area and average of the absolute value of load voltage)

As stated before, the data matrix that used for the identification task is 440 raw × 13 columns. In this work, 50% of the data 220 × 13 are used for train the LVQ algorithm and remaining are used for validate and test the algorithm share equally. As shown in Figure 5.3 to 5.14, it is clear that the similarity between the PDF and SHF with the IDF features. Thus, the classification algorithm should be worked in four levels due to this similarity. Figure 5.15 show the logic flow chart that describe the fault classification.

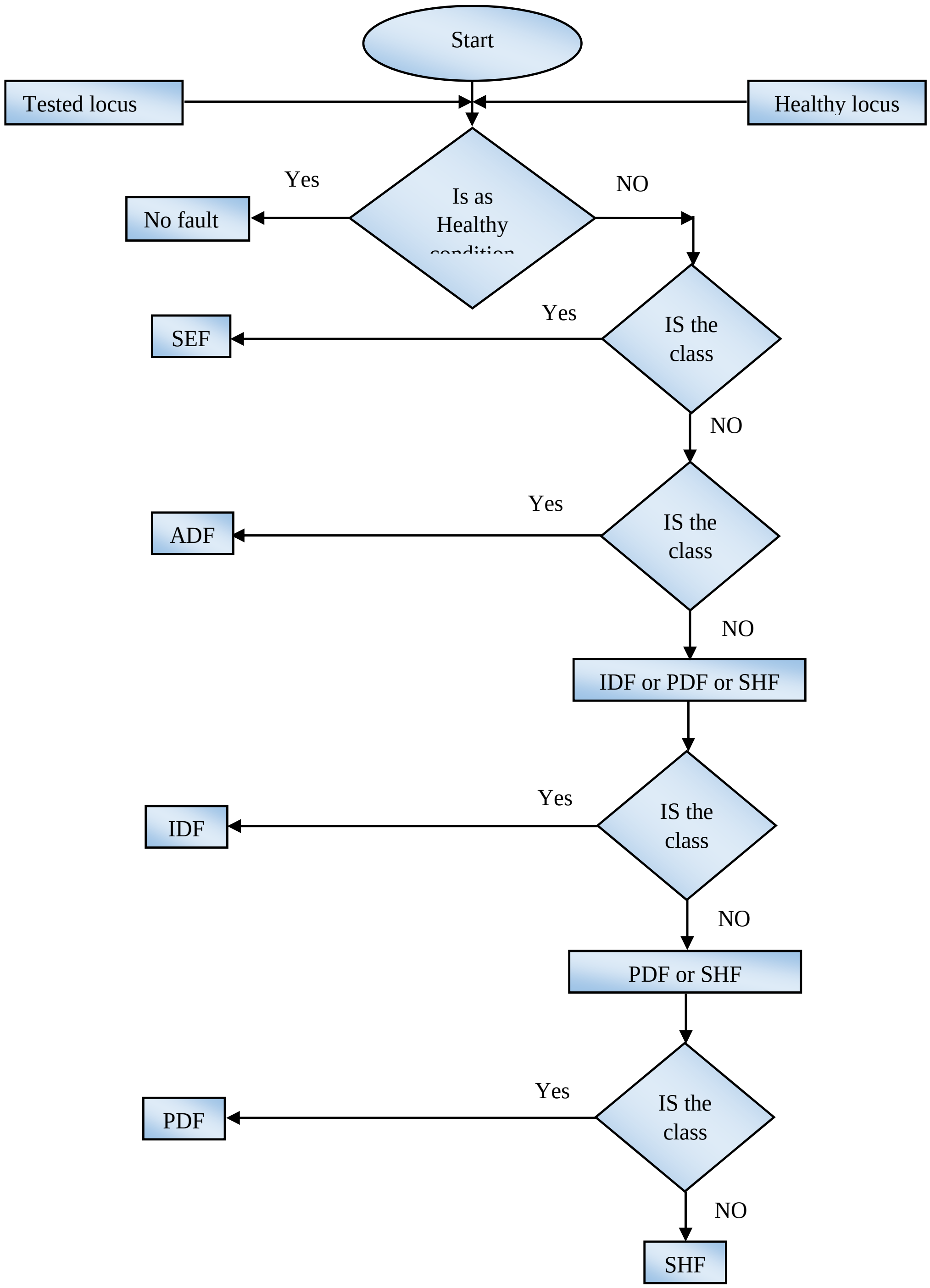

Figure 5.15. Fault identification flow chart

The first level identifies the type of insulation failure, viz. ‘series fault’ (SEF) or ‘axial displacement fault’ (ADF) or any type of ‘partial discharge’ (PDF),‘shunt short circuit’ (SHF) and ‘inter disk fault’ (IDF). The first level output is “1” for SEF, “2” for IDF or PDF or SHF, and “3” for ADF. Figure 5.16 showing the errors in the first network, illustrates that the network was able to achieve near perfect classification of the validation data, with the sum squared error of the output data being in the order of 0.0808 at time 1 sec. and 29 min.

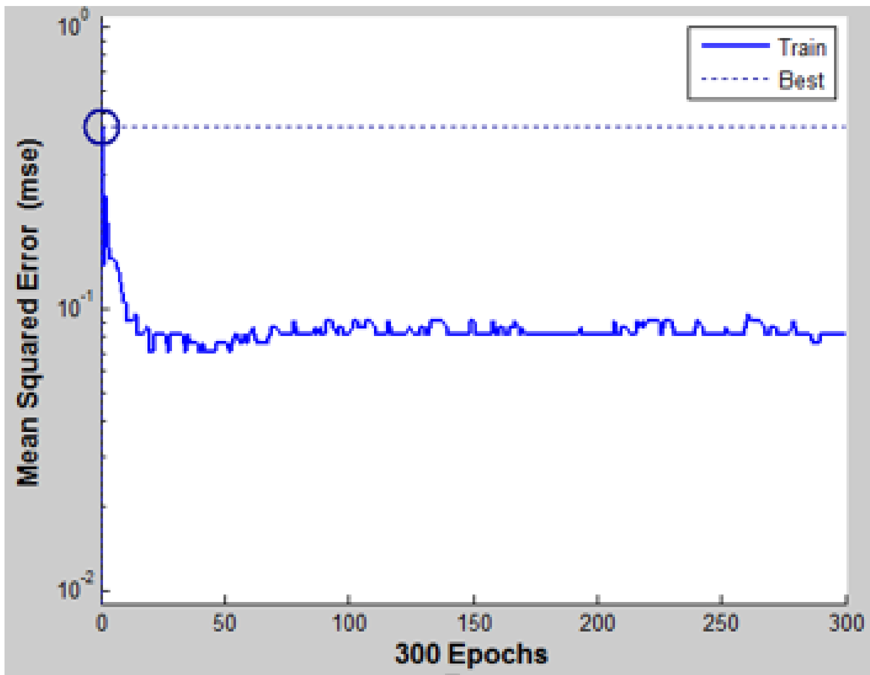

Figure 5.16: Errors in layer one classification of validation data

All training values of features for SEF, IDF, and ADF can be used directly as an inputs to the first classifier network. So, in total the data set matrix that used for fault identification based on learn vector quantization LVQ has form 44×3= 132 case (row) and 13 features (column). If the output of the first level is “2”, this means that the fault type may be IDF or PDF or SHF. And that chivied by the second level of classification. In the second level, the network identifies the type of insulation failure, viz. ‘inter disk fault’ (IDF) or any type of ‘partial discharge’ (PDF), and ‘shunt short circuit’ (SHF). The second level output is “1” for IDF and “2” for PDF or SHF. In the second network the performance goal met after only one of 100 epochs and this takes one sec. so the overall time of the first and second network that able to achieve near perfect classification of the validation data is 1 min and 30 sec. the features that used as inputs to the second network are all features values of IDF and PDF. This values forms 44×2= 88 case (row) and 13 features. If the output of the second network is “2”, this means that the type of fault may be PDF or SHF. The fault can be identified either as (PDF) or (SHF) by the third level. The output of the third network is “1” for the PDF type and “2” for the SHF type. In this level of classifier we use only features number 11, 12 and 13 of PDF and SHF as an input to train this network. This values forms 44×2= 88 case (row) and 3 features. The minor similarity between SEF and IDF will effect on the accuracy if we use only three level. Thus, forth level is used to increase the whole accuracy. In The fourth level, we use the probabilistic neural network. In this level we use only SESC and ADF features as an input to train this network. With these classifier levels, the ANN algorithm successfully for identify the insulation winding failure under any type of the proposed fault condition.

As mentioned before, for insulation failure identification, thirteen significant features are extracted from each of 440 locus. Among that, 50% of the data are used as a training samples. While the remaining 50% of the data samples are used to validate and test the identification accuracy of LVQ algorithm. This algorithm has successfully identified 432 fault loci from 440 total faulty loci after 1 min and 32 sec by using 13 features. Thus, an entire identification accuracy of about 98.1818% has been obtained from this identification algorithm. Figure 5.17, 5.18, 5.19, 5.20, and 5.21 shows the actual and predicted locus when we test the algorithm at different fault locations with all types of faults. The fault identification accuracies of the proposed algorithm are given in table 5.1.

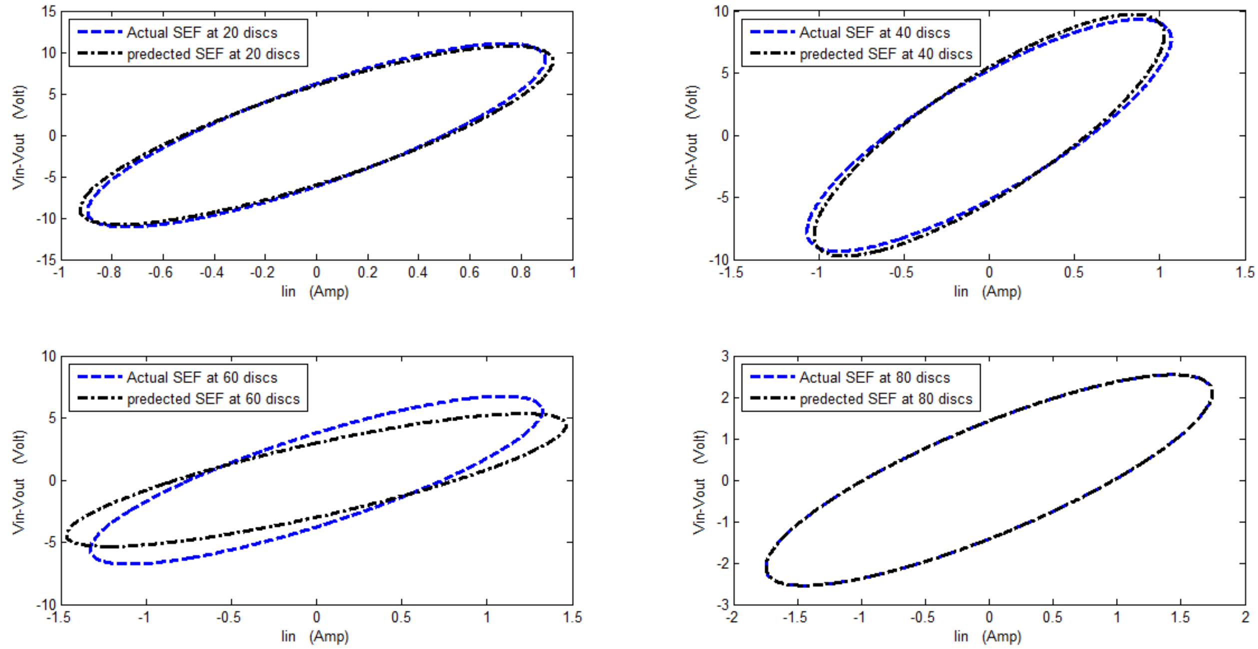

Figure 5.17. Actual and predicted locus when we test the algorithm at different fault locations SEF type

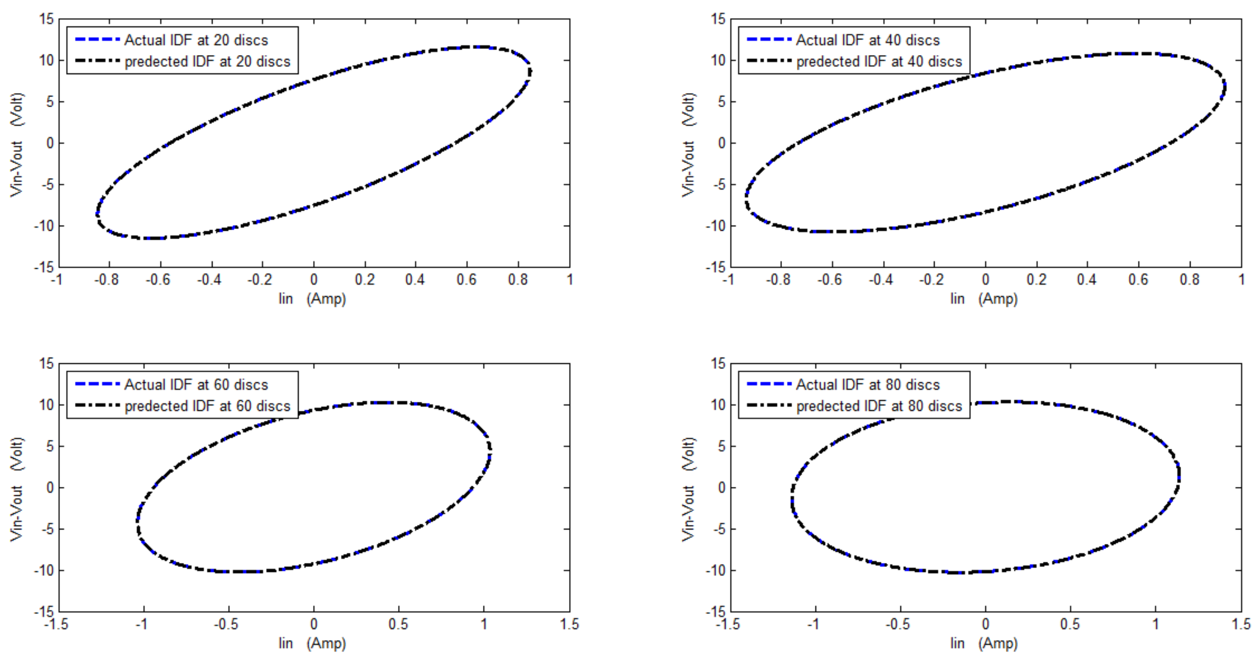

Figure 5.18. Actual and predicted locus when we test the algorithm at different fault locations IDF type

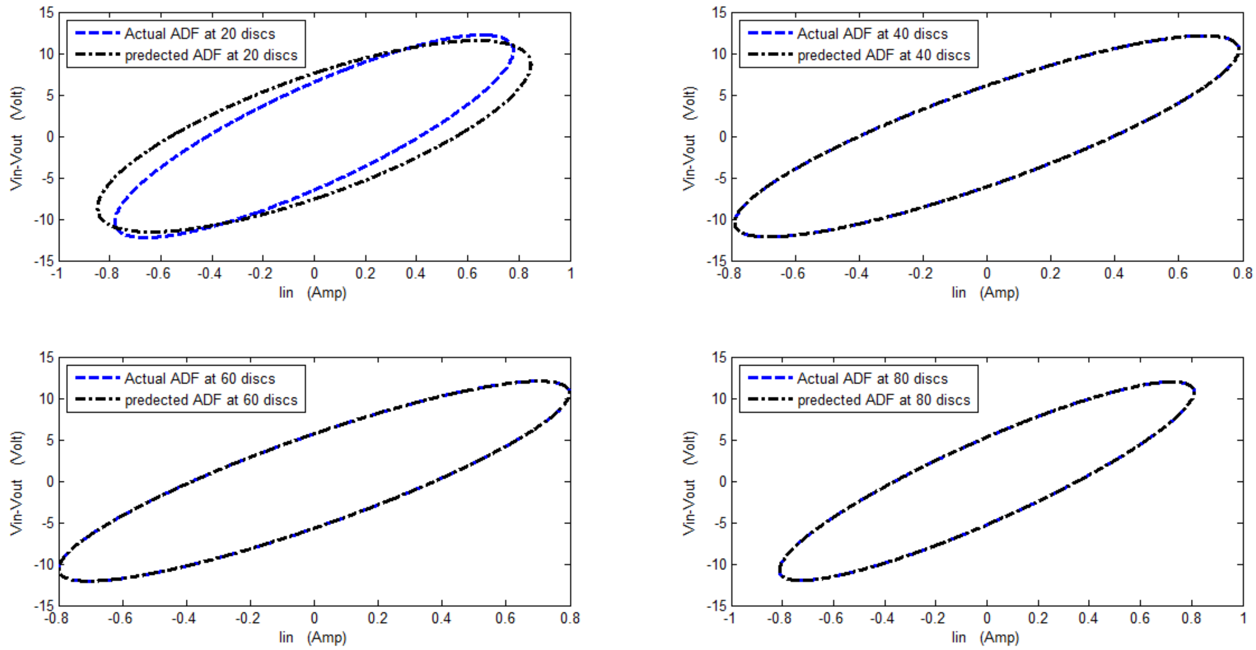

Figure 5.19. Actual and predicted locus when we test the algorithm at different fault locations ADF type

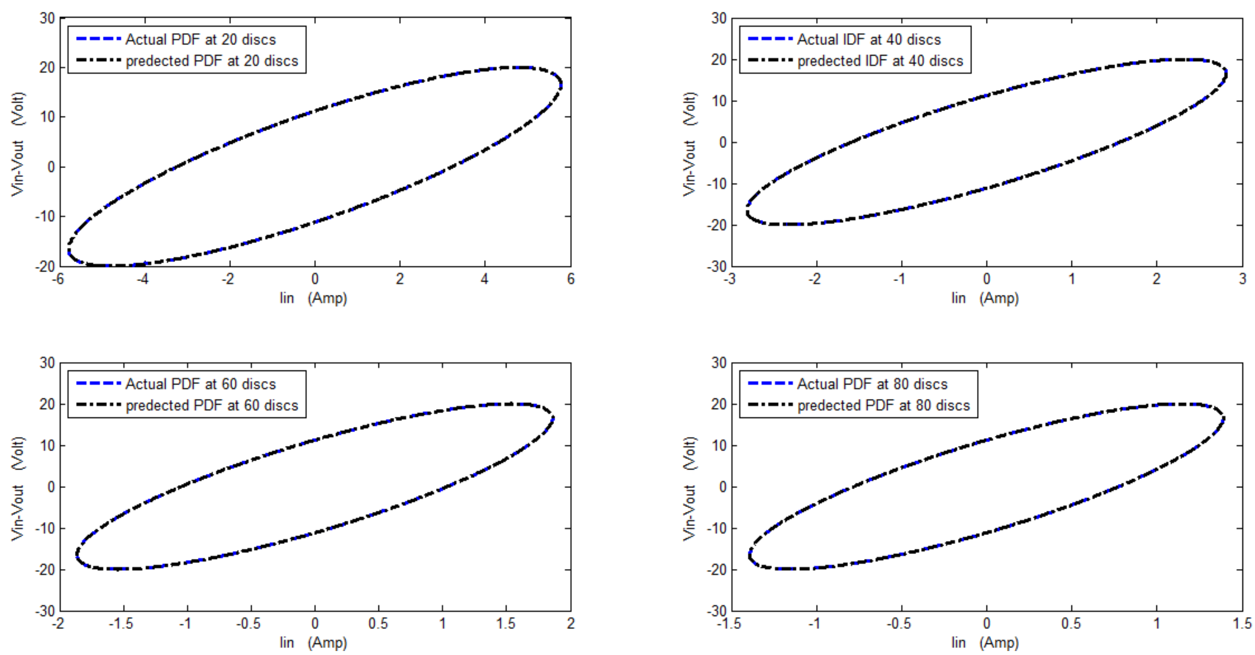

Figure 5.20. Actual and predicted locus when we test the algorithm at different fault locations PDF type

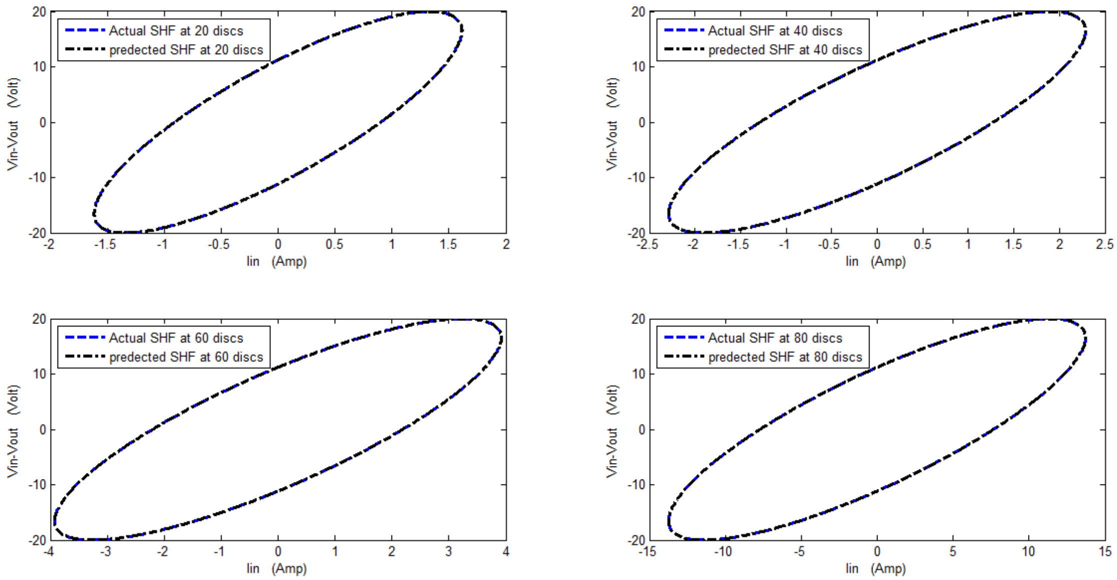

Figure 5.21. Actual and predicted locus when we test the algorithm at different fault locations SHF type

Table 5.1. Confusion matrix showing identification accuracy of train, validation and test data points

		Predicted cases							
		SEF	IDF	ADF	PDF	SHF	No. of obj.	Accuracy	Over all Accuracy
Training	SEF	44	0	0	0	0	44	100%	100%
	IDF	0	44	0	0	0	44	100%	
	ADF	0	0	44	0	0	44	100%	
	PDF	0	0	0	44	0	44	100%	
	SHF	0	0	0	0	44	44	100%	
validation	SEF	20	1	1	0	0	22	90.91%	95.45%
	IDF	0	22	0	0	0	22	100%	
	ADF	0	1	21	0	0	22	95.45%	
	PDF	1	0	0	20	1	22	90.91%	
	SHF	0	0	0	0	22	22	100%	
Testing	SEF	21	0	1	0	0	22	95.45%	97.27%
	IDF	0	22	0	0	0	22	100%	
	ADF	0	0	22	0	0	22	100%	
	PDF	0	0	0	21	1	22	95.45%	
	SHF	1	0	0	0	21	22	95.45%	

CONCLUSION

The simulation of five different types of insulation failures in PSIM based model of 33 KV winding, 3MVA power transformer is undertaken. Successful discrimination between these insulation failures was performed utilizing a neural network approach. The input voltage - output voltage and input currents are utilized to construct the (ΔV- I_{in}) locus. The change in the (ΔV- I_{in}) locus for different types of insulation failure was constructed. A multi-level neural network approach based on analytical features training sets was developed to identify such deformations in power transformers. The system comprised three learn vector quantization levels in addition to a probabilistic neural network level in order to discriminate between all types of faults efficiently.

The fault identification results based on the used algorithm show that thirteen features are sufficient to get a reasonably good accuracy in the identification task. The proposed algorithm has successfully identified 432 fault loci from 440 total faulty loci after 1 min and 32 sec by using the extracted features. The results showed that the developed classifier has successfully identified and localized all five different types of insulation failures within ± 4.55% winding length with acceptable accuracy of about 98.1818%.

Such a system would be a useful tool for preventive maintenance of transformers enabling power management system to spot the ones requiring immediate periodic maintenance or exchange without the interruption of supply. Integrate this study into studying the performance of an online internal transformer fault detection approach for non-sinusoidal operating conditions (that produced due to noise and harmonics), and developing an overall smart automated tool that localized the internal condition of the transformers under this conditions.

REFERENCES

[1] KUllal Ray, P Rajamani and Abhijit Mukherjee, "K-Nearest Neighbor Algorithm Based Classification and Localization of Seven Different Types of Disc-to-Disc Impulse Insulation Failures in Power Transformer, " IEEE 10th International Conference on the Properties and Applications of Dielectric Materials, Bangalore, India, pp. 1-5, 2012.

[2] H. Tavakoli, "A High Frequency Transformer Winding Model for FRA Applications", M.Sc. Thesis, Division of Electromagnetic Engineering, KTH School of Electrical Engineering, Sweden, pp.13-18, 2009.

[3] C.Koley, P.Purkait and S.Chakravorti, "Wavelet-aided SVM tool for impulse fault identification in transformers," IEEE Trans. on Power Delivery, Vol.2l, NO.3, pp.1283-1290, July 2006.

[4] P.Rajamani, S.Chakravorti, "Identification of simultaneously occurring dynamic disc to disc insulation failures in transformer winding under impulse excitation," IEEE Trans. on Dielectr. and Electr. Insul., VoLl9, No.2, pp 443-453, 2012.

[5] V.Jeyabalan and S.Usa, "Frequency Domain Correlation Technique for PD Location in Transformer winding," IEEE Trans. on Dielectr. and Electr. Insul., VoLl6, pp. 1160-1167, August 2009.

[6] E. Kuffel, W. S. Zaengl, "High Voltage Engineering Fundamentals", Pergamon Press, pp. 478-480, 1983.

[7] B. Augustein, W. Fox, and P. Fischer, “Outsourced monitoring and reliability of critical assets,” tech. rep., Distributech, Severon Corporation, 2003.

[8] C. Newton, "The Future of Large Power Transformers", Transmission & Distribution World, http;//tdworld.com/ar/power_future large_power/, Sept. 1997.

[9] CIGRE Working Group 05, "An International Survey on Failures in Large Power Transformers in Service", Electra, No. 88, May 1983.

[10] F. Tanguay, "Transformer Maintenance: The Cheapest Form of Insurance Parti: The Transformer Killers", Electricity Today No. 1, pp. 5-9, 2002.

[11] Arvind Singh, "High Frequency Simulation of Transformer Windings for Diagnostic Tests", M.Sc. Thesis, Electrical and Computer Engineering, The University of British Colombia, February 2006.

[12] D. Allan, H. Moore, Eelectric Power Transformer Engineering,nCRC Press LLC, FL, USA, 2004.

[13] A. C. Franklin, D. P. Franklin, The J&P Transformer Book: A Practical Technology of The Power Transformer, pp. 629, 11th Edition, Butterworth & Co. Ltd., 1983.

[14] P. M. Joshi and S. V. Kulkarni, "Transformer winding diagnostics using deformation coefficient", IEEE Power and Energy Soc., General Meeting, Conversion and Delivery of Electrical Energy in the 21st Century, pp. 1-4, 2008.

[15] IEEE Guide for Diagnostic Field Testing of Electric Power Apparatus, Part 1: Oil Filled Power Transformers, Regulators, and Reactors, IEEE Std 62-1995.

[16] Trafo Union Co.,“Transformer design documents”, TUB 27000.01.0 and 27100.10.0. Germany.

[17] M. Florkowski, "Exploitation stresses and challenges in diagnostics of electrical industrial equipment", IEEE Int’l. Sympos. Industrial Electronics (ISIE), pp. 15-25, 2011.

[18] M. Florkowski and J. Furgal, "Identification of winding faults in electric machines using a high frequency method", IEEE Int’l. Conf. Electric Machines & Drives (IEMDC), pp. 590-

595, 2007.

[19] J. R. Secue and E. Mombello, "Sweep frequency response analysis (SFRA) for the assessment of winding displacements and deformation in power transformers", Electric Power Syst. Research, Vol. 78, pp. 11191128, 2008

[20] M. Wang, A. J. Vandermaar and K. D. Srivastava, "Improved etection of power transformer winding movement by extending the FRA high frequency range", IEEE Trans. Power Del., Vol. 20, pp. 1930-1938, 2005.

[21] B. García, J.C. Burgos and A.M. Alonso, "Winding deformations detection in power transformers by tank vibrations monitoring", Electric Power Syst. Research, Vol. 74, pp. 129-138, 2004.

[22] B. García, J.C. Burgos and A.M. Alonso, "Transformer tank vibration modeling as a method of detecting winding deformationspart I: theoretical foundation", IEEE Trans. Power Del., Vol. 21, pp. 157-163, 2006.

[23] B. García, J.C. Burgos and A.M. Alonso, "Transformer tank vibration modeling as a method of detecting winding deformations part II: experimental verification", IEEE Trans. Power Del., Vol. 21, pp. 164-169, 2006.

[24] M.A. Hejazi, M. Choopani, M. Dabir and G.B. Gharehpetian, "Effect of antenna position on on-line monitoring of transformer winding axial displacement using electromagnetic waves", IEEE 2nd Int'l. Power Energy Conf. (PECon), pp. 44-49, 2008.

[25] M. Akhavanhejazi, G.B. Gharehpetian, R. Faraji-Dana, G.R. Moradi, M. Mohammadi and H.A. Alehoseini, "A new on-line monitoring method of transformer winding axial displacement based on measurement of scattering parameters and decision tree", Expert Syst. Applications, Vol. 38, pp. 8886-8893, 2011.

[26] M. A. Hejazi, G. B. Gharehpetian, G. Moradi, H. A. Alehosseini and M. Mohammadi, "Online monitoring of transformer winding axial displacement and its extent using scattering parameters and knearest neighbor method", IET Proc. Generation, Transmission Distribution, Vol. 5, pp. 824-832, 2011.

[27] P. M. Joshi and S. V. Kulkarni, "A novel approach for online deformation diagnostics of transformer windings”, IEEE Power and Energy Society, General Meeting, pp. 1-6, 2010.

[28] N. Shu, C. Zhou, F. Hu, Q. Liu and L. Zheng, "Study on ultrasonic measurement device for transformer winding deformation", IEEE Int’l. Conf. Power Syst. Techn., (POWERCON), Vol.3, pp. 1401- 1404, 2002.

[29] T.Babnik, R.Aggarwal and P.Moore, "Data Mining on a Transformer Partial Discharge Data Using the Self-organizing Map," IEEE Transactions on Dielectrics and Electrical Insulation, vol. 14, no. 2, pp. 444-452, April 2007.

[30] A.A.Mazroua, R.Bartnikas and M.M.A. Salama, "Discrimination Between PD Pulse Shapes using Different Neural Network Paradigms," IEEE Transactions on Dielectrics and Electrical Insulation, vol. 1, no. 6, pp. 1119-1131, Dec. 2004.

[31] Feng Yan, Wenxuan Liu, Lin Tian, “A New Neural Network Approach for Fault Location of Distribution Network ", IEEE Int. Conf. on Mechatronic Science, Electric Engineering and Computer, pp. 1344- 1347, 2011.

[32] Jianye Liu, Yongchun Liang, Xiaoyun Sun, “Application ofLeaming Vector Quantization Network in Fault Diagnosis of Power Transformer ", IEEE Int. Conf. on Mechatronic and Automation, pp. 4435- 4439, 2009.

[33] S. M. H. Hosseini, M. Vakilian, and G. B. Gharehpetian, “Comparison of Transformer Detailed Models for Fast and Very Fast Transient Studies” IEEE Trans. Power Delivery, Vol. 23, No. 2, April 2008, pp. 733-741.

[34] C. K. Roy and J. R. Biswas, "Studies on impulse behavior of a transformer winding with simulated faults by analogue modeling," Proc. Inst. Elect. Eng., C, vol. 141, pp. 401–412, 1994.

[35] Z. D. Wang, S. N. Hettiwatte, and P. A, Crossley, "A measurements based discharge location algorithm for plain disc winding power transformers," IEEE Trans. On Dielectrics and Electrical Insulation, Vol. 12, Issue. 3, June 2005, pp. 416-422.

[36] K. X. Lai, "Application of data mining techniques for characterization and recognition of partial discharge," PhD Thesis, Department of Electric Power Engineering, University of New South Wales, Sydney, 2010.

[37] Ari, N. and Blumer, W.; Transient Electromagnetic Fields Due to Switching Operations in Electric Power Systems; IEEE Trans. On Electromagnetic Compatibility, Vol.: EMC-29, No.: 3, Page(s): 233 – 237, 1987.

[38] J. Chong and A. Abu-Siada, "A Novel Algorithm to detect Internal Transformer Faults," in Power and Energy Society General Meeting IEEE, Australia-Western, 2011, pp. 1-5.

[39] S. M. Islam and G. Ledwich, "Locating transformer faults through sensitivity analysis of high frequency modeling using transfer function approach," in Electrical Insulation, 1996., Conference Record of the 1996 IEEE International Symposium on, 1996, pp. 38-41 vol.1.

[40] M. F. El-Naggar, A. M. Hamdy, S. M. Moussa, and E. El-Din, "A novel approach for fault diagnosis of power transformers based on extracting invariant moments," in Power Engineering Conference, 2008. AUPEC '08. Australasian Universities, 2008, pp. 1-5.

[41] Sophocles J. Orfanidis, Electromagnetic Waves and Antennas, Rutgers University.

[42] G. B. Thomas and R. L. Finney, Calculus and Analytic Geometry, 9th ed. Reading, MA: Addison-Wesley, 1996.

APPENDIX

MATLAB CODEs:

1. ANN classification code.

```
clear all
close all
clc

ALL_FEATURES_DATA=xlsread('ALL FEATURES DATA.xlsx');
SESC=ALL_FEATURES_DATA(:,[1:13]);
IDF=ALL_FEATURES_DATA(:,[14:26]);
ADF=ALL_FEATURES_DATA(:,[27:39]);
PDF=ALL_FEATURES_DATA(:,[40:52]);
SHSC=ALL_FEATURES_DATA(:,[53:65]);

test_no=[];
validation_no=[];
train_no=[];
for i=4:4:88
    test_no=[test_no i];
    validation_no=[validation_no i-3];
    train_no=[train_no i-2 i-1];
end

% Train Data %
SESC_train=SESC(train_no,:);
IDF_train=IDF(train_no,:);
ADF_train=ADF(train_no,:);
PDF_train=PDF(train_no,:);
SHSC_train=SHSC(train_no,:);

% Validation Data %
SESC_validation=SESC(validation_no,:);
IDF_validation=IDF(validation_no,:);
ADF_validation=ADF(validation_no,:);
PDF_validation=PDF(validation_no,:);
SHSC_validation=SHSC(validation_no,:);

% Test Data %
SESC_test=SESC(test_no,:);
IDF_test=IDF(test_no,:);
ADF_test=ADF(test_no,:);
PDF_test=PDF(test_no,:);
SHSC_test=SHSC(test_no,:);

% ANN#1 to identify class 1 (for SESC) or 2 (for IDF or PDF or SHSC) or 3
(for ADF) %
P=[SESC_train' IDF_train' ADF_train'];
```

```
t1=ones(1,44);t2=ones(1,44)*2;t3=ones(1,44)*3;t4=ones(1,44)*4;t5=ones(1,44)
*5;
Tc=[ t1 t2 t3 ];
T = ind2vec(Tc);
targets = full(T);
net = lvqnet(30);
net = configure(net,P,T);
net.trainParam.epochs = 1000;

net = train(net,P,T);



Yc11 = vec2ind(net([SESC_train']));
Yc21 = vec2ind(net([IDF_train']));
Yc31 = vec2ind(net([ADF_train']));
Yc41 = vec2ind(net([PDF_train']));
Yc51 = vec2ind(net([SHSC_train']));

Yc1=[Yc11;Yc21;Yc31;Yc41;Yc51]; % (5*44) output of ANN#1 by using input
train no

% ANN#2 to identify class 1 (for IDF) or 2 (for PDF or SHSC) %
P1=[  IDF_train' PDF_train' ];
P1=P1((11:end),:);
Tc1=[ t1 t2 ];
T1 = ind2vec(Tc1);
targets1 = full(T1);
net1 = lvqnet(10);
net1 = configure(net1,P1,T1);
net.trainParam.epochs = 100;
net1 = train(net1,P1,T1);
Yc21_1 = vec2ind(net1([IDF_train(:,(11:end))]'));
Yc41_1 = vec2ind(net1([PDF_train(:,(11:end))]'));
Yc51_1 = vec2ind(net1([SHSC_train(:,(11:end))]'));

% ANN#3 to identify class 1 (for PDF) or 2 (for SHSC) %
P2=[  PDF_train' SHSC_train' ];
P2=P2((11:end),:);
Tc2=[ t4 t5 ];
T2 = ind2vec(Tc2);
targets2 = full(T2);
net2 = lvqnet(10);
net2 = configure(net2,P2,T2);
net.trainParam.epochs = 100;
net2 = train(net2,P2,T2);
Yc41_2 = vec2ind(net2([PDF_train(:,(11:end))]'));
Yc51_2 = vec2ind(net2([SHSC_train(:,(11:end))]'));

% ANN#4 to identify class 1 (for SESC) or 2 (for ADF) %
P3=[SESC_train' ADF_train'];
t1=ones(1,44);t2=ones(1,44)*2;t3=ones(1,44)*3;t4=ones(1,44)*4;t5=ones(1,44)
*5;
Tc3=[ t1 t3];
T3 = ind2vec(Tc3);
net3 = newpnn(P3,T3);
```

```
Y = sim(net3,P3);
Yc = vec2ind(Y)
Yc11_3 = vec2ind(sim(net3,[SESC_train']));
Yc31_3 = vec2ind(sim(net3,[ADF_train']));

Yc_train=[Yc11_3;Yc21;Yc31_3;Yc41_2;Yc51_2]

Yc12 = vec2ind(net([SESC_validation']));
Yc22 = vec2ind(net([IDF_validation']));
Yc32 = vec2ind(net([ADF_validation']));
Yc42 = vec2ind(net([PDF_validation']));
Yc52 = vec2ind(net([SHSC_validation']));

Yc_validation=[Yc12;Yc22;Yc32;Yc42;Yc52];

Yc13 = vec2ind(net([SESC_test']));
Yc23 = vec2ind(net([IDF_test']));
Yc33 = vec2ind(net([ADF_test']));
Yc43 = vec2ind(net([PDF_test']));
Yc53 = vec2ind(net([SHSC_test']));

Yc_test=[Yc13;Yc23;Yc33;Yc43;Yc53];

for i=1:5
    for j=1:22
        if Yc_validation(i,j)==2&i==1
            PB=SESC_validation';
            PA=PB(:,j);
            Y=vec2ind(net1(PA((11:end),:)));
            if Y==1
                Yc_validation(i,j)=2;
            else
                Z=vec2ind(net2(PA((11:end),:)));
                if Z==4
                    Yc_validation(i,j)=4;
                else
                    Yc_validation(i,j)=5;
                end
            end
        elseif Yc_validation(i,j)==2&i==2
            PB=IDF_validation';
            PA=PB(:,j);
            Y=vec2ind(net1(PA((11:end),:)));
            if Y==1
                Yc_validation(i,j)=2;
            else
                Z=vec2ind(net2(PA((11:end),:)));
                if Z==4
                    Yc_validation(i,j)=4;
                else
                    Yc_validation(i,j)=5;
                end
            end
        elseif Yc_validation(i,j)==2&i==3
            PB=ADF_validation';
            PA=PB(:,j);
```

```
            Y=vec2ind(net1(PA((11:end),:)));
            if Y==1
                Yc_validation(i,j)=2;
            else
                Z=vec2ind(net2(PA((11:end),:)));
                if Z==4
                    Yc_validation(i,j)=4;
                else
                    Yc_validation(i,j)=5;
                end
            end
        elseif Yc_validation(i,j)==2&i==4
            PB=PDF_validation';
            PA=PB(:,j);
            Y=vec2ind(net1(PA((11:end),:)));
            if Y==1
                Yc_validation(i,j)=2;
            else
                Z=vec2ind(net2(PA((11:end),:)));
                if Z==4
                    Yc_validation(i,j)=4;
                else
                    Yc_validation(i,j)=5;
                end
            end
        elseif Yc_validation(i,j)==2&i==5
            PB=SHSC_validation';
            PA=PB(:,j);
            Y=vec2ind(net1(PA((11:end),:)));
            if Y==1
                Yc_validation(i,j)=2;
            else
                Z=vec2ind(net2(PA((11:end),:)));
                if Z==4
                    Yc_validation(i,j)=4;
                else
                    Yc_validation(i,j)=5;
                end
            end
        end
    end
end


for i=1:5
    for j=1:22
        if Yc_test(i,j)==2&i==1
            PB=SESC_test';
            PA=PB(:,j);
            Y=vec2ind(net1(PA((11:end),:)));
            if Y==1
                Yc_test(i,j)=2;
            else
                Z=vec2ind(net2(PA((11:end),:)));
                if Z==4
                    Yc_test(i,j)=4;
```

```
        else
            Yc_test(i,j)=5;
        end
    end
elseif Yc_test(i,j)==2&i==2
    PB=IDF_test';
    PA=PB(:,j);
    Y=vec2ind(net1(PA((11:end),:)));
    if Y==1
        Yc_test(i,j)=2;
    else
        Z=vec2ind(net2(PA((11:end),:)));
        if Z==4
            Yc_test(i,j)=4;
        else
            Yc_test(i,j)=5;
        end
    end
elseif Yc_test(i,j)==2&i==3
    PB=ADF_test';
    PA=PB(:,j);
    Y=vec2ind(net1(PA((11:end),:)));
    if Y==1
        Yc_test(i,j)=2;
    else
        Z=vec2ind(net2(PA((11:end),:)));
        if Z==4
            Yc_test(i,j)=4;
        else
            Yc_test(i,j)=5;
        end
    end
elseif Yc_test(i,j)==2&i==4
    PB=PDF_test';
    PA=PB(:,j);
    Y=vec2ind(net1(PA((11:end),:)));
    if Y==1
        Yc_test(i,j)=2;
    else
        Z=vec2ind(net2(PA((11:end),:)));
        if Z==4
            Yc_test(i,j)=4;
        else
            Yc_test(i,j)=5;
        end
    end
elseif Yc_test(i,j)==2&i==5
    PB=SHSC_test';
    PA=PB(:,j);
    Y=vec2ind(net1(PA((11:end),:)));
    if Y==1
        Yc_test(i,j)=2;
    else
        Z=vec2ind(net2(PA((11:end),:)));
        if Z==4
            Yc_test(i,j)=4;
        else
```

```
                    Yc_test(i,j)=5;
                end
            end
        end
    end
end
```

```
for i=1:5
    for j=1:22
        if (Yc_validation(i,j)==1&i==1)|(Yc_validation(i,j)==3&i==1)
            PB=SESC_validation';
            PA=PB(:,j);
            Y=vec2ind(net3(PA((1:end),:)));
            if Y==1
                Yc_validation(i,j)=1;
            else
                Yc_validation(i,j)=3;
            end
        elseif (Yc_validation(i,j)==1&i==2)|(Yc_validation(i,j)==3&i==2)
            PB=IDF_validation';
            PA=PB(:,j);
            Y=vec2ind(net3(PA((1:end),:)));
            if Y==1
                Yc_validation(i,j)=1;
            else
                Yc_validation(i,j)=3;
            end
        elseif (Yc_validation(i,j)==1&i==3)|(Yc_validation(i,j)==3&i==3)
            PB=ADF_validation';
            PA=PB(:,j);
            Y=vec2ind(net3(PA((1:end),:)));
            if Y==1
                Yc_validation(i,j)=1;
            else
                Yc_validation(i,j)=3;
            end
        elseif (Yc_validation(i,j)==1&i==4)|(Yc_validation(i,j)==3&i==4)
            PB=PDF_validation';
            PA=PB(:,j);
            Y=vec2ind(net3(PA((1:end),:)));
            if Y==1
                Yc_validation(i,j)=1;
            else
                Yc_validation(i,j)=3;
            end
        elseif (Yc_validation(i,j)==1&i==5)|(Yc_validation(i,j)==3&i==5)
            PB=SHSC_validation';
            PA=PB(:,j);
            Y=vec2ind(net3(PA((1:end),:)));
            if Y==1
                Yc_validation(i,j)=1;
```

```
            else

            end
        end
    end
end


for i=1:5
    for j=1:22
        if (Yc_test(i,j)==1&i==1)|(Yc_test(i,j)==3&i==1)
            PB=SESC_test';
            PA=PB(:,j);
            Y=vec2ind(net3(PA((1:end),:)));
            if Y==1
                Yc_test(i,j)=1;
            else
                Yc_test(i,j)=3;
            end
        elseif (Yc_test(i,j)==1&i==2)|(Yc_test(i,j)==3&i==2)
            PB=IDF_test';
            PA=PB(:,j);
            Y=vec2ind(net3(PA((1:end),:)));
            if Y==1
                Yc_test(i,j)=1;
            else
                Yc_test(i,j)=3;
            end
        elseif (Yc_test(i,j)==1&i==3)|(Yc_test(i,j)==3&i==3)
            PB=ADF_test';
            PA=PB(:,j);
            Y=vec2ind(net3(PA((1:end),:)));
            if Y==1
                Yc_test(i,j)=1;
            else
                Yc_test(i,j)=3;
            end
        elseif (Yc_test(i,j)==1&i==4)|(Yc_test(i,j)==3&i==4)
            PB=PDF_test';
            PA=PB(:,j);
            Y=vec2ind(net3(PA((1:end),:)));
            if Y==1
                Yc_test(i,j)=1;
            else
                Yc_test(i,j)=3;
            end
        elseif (Yc_test(i,j)==1&i==5)|(Yc_test(i,j)==3&i==5)
            PB=SHSC_test';
            PA=PB(:,j);
            Y=vec2ind(net3(PA((1:end),:)));
            if Y==1
                Yc_test(i,j)=1;
            else

            end
        end
```

```
    end
end



Yc_validation
Yc_test
Yc_overall=[Yc_train Yc_validation Yc_test];

acc_train=((length(find(Yc_train(1,:)==1))+length(find(Yc_train(2,:)==2))+l
ength(find(Yc_train(3,:)==3))+length(find(Yc_train(4,:)==4))+length(find(Yc
_train(5,:)==5)))/(length(find(Yc_train(1,:)))+length(find(Yc_train(2,:)))+
length(find(Yc_train(3,:)))+length(find(Yc_train(4,:)))+length(find(Yc_trai
n(5,:)))))*100
acc_validation=((length(find(Yc_validation(1,:)==1))+length(find(Yc_validat
ion(2,:)==2))+length(find(Yc_validation(3,:)==3))+length(find(Yc_validation
(4,:)==4))+length(find(Yc_validation(5,:)==5)))/(length(find(Yc_validation(
1,:)))+length(find(Yc_validation(2,:)))+length(find(Yc_validation(3,:)))+le
ngth(find(Yc_validation(4,:)))+length(find(Yc_validation(5,:)))))*100
acc_test=(length(find(Yc_test(1,:)==1))+length(find(Yc_test(2,:)==2))+lengt
h(find(Yc_test(3,:)==3))+length(find(Yc_test(4,:)==4))+length(find(Yc_test(
5,:)==5)))/(length(find(Yc_test(1,:)))+length(find(Yc_test(2,:)))+length(fi
nd(Yc_test(3,:)))+length(find(Yc_test(4,:)))+length(find(Yc_test(5,:))))*10
0
acc_overall=((length(find(Yc_overall(1,:)==1))+length(find(Yc_overall(2,:)=
=2))+length(find(Yc_overall(3,:)==3))+length(find(Yc_overall(4,:)==4))+leng
th(find(Yc_overall(5,:)==5)))/(length(find(Yc_overall(1,:)))+length(find(Yc
_overall(2,:)))+length(find(Yc_overall(3,:)))+length(find(Yc_overall(4,:)))
+length(find(Yc_overall(5,:)))))*100
```

The program output is:

```
acc_train =

   100


acc_validation =

   95.4545


acc_test =

   97.2727


acc_overall =

   98.1818
```

2. Code to draw the five classes.

```
clear all
close all
clc

format long

IDF=xlsread('IDF.xlsx');
SESC=xlsread('SESC.xlsx');
ADF=xlsread('ADF.xlsx');
PDF=xlsread('PDF.xlsx');
SHSC=xlsread('SHSC.xlsx');

%_______________________________________________________________________



%_______________________________________________________________________

figure1 = figure('Color',[1 1 1]);
plot(IDF(:,1),IDF(:,2),'+')
hold on
plot(SESC(:,1),SESC(:,2),'OK')
plot(ADF(:,1),ADF(:,2),'OR')
plot(PDF(:,1),PDF(:,2),'O')
plot(SHSC(:,1),SHSC(:,2),'*K')
xlabel('Ellipse area')
ylabel('Angle between the semi-major axis, and the horizontal axis (Theta)
')
axis([0 1000 50 90])
legend('IDF (class 1)','SEF (class 2)','ADF (class 3)', 'PDF (class
4)','SHF (class 5)',4)

%_______________________________________________________________________

figure2 = figure('Color',[1 1 1]);
plot(IDF(:,1),IDF(:,3),'+')
hold on
plot(SESC(:,1),SESC(:,3),'OK')
plot(ADF(:,1),ADF(:,3),'OR')
plot(PDF(:,1),PDF(:,3),'O')
plot(SHSC(:,1),SHSC(:,3),'*K')
xlabel('Ellipse area')
ylabel('Ellipse circumference')
axis([50 400 50 90])
legend('IDF (class 1)','SEF (class 2)','ADF (class 3)','PDF (class 4)','SHF
(class 5)',4)
% %_______________________________________________________________________

figure3 = figure('Color',[1 1 1]);
plot(IDF(:,1),IDF(:,4),'+')
hold on
plot(SESC(:,1),SESC(:,4),'OK')
```

```
plot(ADF(:,1),ADF(:,4),'OR')
plot(PDF(:,1),PDF(:,4),'O')
plot(SHSC(:,1),SHSC(:,4),'*K')
xlabel('Ellipse area')
ylabel('Semi major axis length')
axis([0 2000 0 50])
legend('IDF (class 1)','SEF (class 2)','ADF (class 3)','PDF (class 4)','SHF
(class 5)',4)
%_______________________________________________________________________

figure4 = figure('Color',[1 1 1]);
plot(IDF(:,1),IDF(:,5),'+')
hold on
plot(SESC(:,1),SESC(:,5),'OK')
plot(ADF(:,1),ADF(:,5),'OR')
plot(PDF(:,1),PDF(:,5),'O')
plot(SHSC(:,1),SHSC(:,5),'*K')
xlabel('Ellipse area')
ylabel('Semi minor axis length')
axis([0 1000 0 12])
legend('IDF (class 1)','SEF (class 2)','ADF (class 3)','PDF (class 4)','SHF
(class 5)',4)

%_______________________________________________________________________

figure5 = figure('Color',[1 1 1]);
plot(IDF(:,1),IDF(:,6),'+')
hold on
plot(SESC(:,1),SESC(:,6),'OK')
plot(ADF(:,1),ADF(:,6),'OR')
plot(PDF(:,1),PDF(:,6),'O')
plot(SHSC(:,1),SHSC(:,6),'*K')
xlabel('Ellipse area')
ylabel('Ellipse focus')
axis([0 1000 -4 40])
legend('IDF (class 1)','SEF (class 2)','ADF (class 3)','PDF (class 4)','SHF
(class 5)',4)
%_______________________________________________________________________

figure6 = figure('Color',[1 1 1]);
plot(IDF(:,1),IDF(:,7),'+')
hold on
plot(SESC(:,1),SESC(:,7),'OK')
plot(ADF(:,1),ADF(:,7),'OR')
plot(PDF(:,1),PDF(:,7),'O')
plot(SHSC(:,1),SHSC(:,7),'*K')
xlabel('Ellipse area')
ylabel('First ellipse eccentricity')
axis([0 1000 -0.4 1])
legend('IDF (class 1)','SEF (class 2)','ADF (class 3)','PDF (class 4)','SHF
(class 5)',4)
%_______________________________________________________________________

figure7 = figure('Color',[1 1 1]);
plot(IDF(:,1),IDF(:,8),'+')
hold on
```

```
plot(SESC(:,1),SESC(:,8),'OK')
plot(ADF(:,1),ADF(:,8),'OR')
plot(PDF(:,1),PDF(:,8),'O')
plot(SHSC(:,1),SHSC(:,8),'*K')
xlabel('Ellipse area')
ylabel('Second ellipse eccentricity')
axis([0 1000 0 10])
legend('IDF (class 1)','SEF (class 2)','ADF (class 3)','PDF (class 4)','SHF
(class 5)')
%__________________________________________________________________________

figure8 = figure('Color',[1 1 1]);
plot(IDF(:,1),IDF(:,9),'+')
hold on
plot(SESC(:,1),SESC(:,9),'OK')
plot(ADF(:,1),ADF(:,9),'OR')
plot(PDF(:,1),PDF(:,9),'O')
plot(SHSC(:,1),SHSC(:,9),'*K')
axis([0 1000 0 1.5])
xlabel('Ellipse area')
ylabel('ratio between first and second ellipse eccentricity')
legend('IDF (class 1)','SEF (class 2)','ADF (class 3)','PDF (class 4)','SHF
(class 5)')
%__________________________________________________________________________

figure9 = figure('Color',[1 1 1]);
plot(IDF(:,1),IDF(:,10),'+')
hold on
plot(SESC(:,1),SESC(:,10),'OK')
plot(ADF(:,1),ADF(:,10),'OR')
plot(PDF(:,1),PDF(:,10),'O')
plot(SHSC(:,1),SHSC(:,10),'*K')
xlabel('Ellipse area')
ylabel('Ellipse flattering')
legend('IDF (class 1)','SEF (class 2)','ADF (class 3)','PDF (class 4)','SHF
(class 5)')
axis([0 1000 0 1.5])
%__________________________________________________________________________

figure10 = figure('Color',[1 1 1]);
plot(IDF(:,1),IDF(:,11),'+')
hold on
plot(SESC(:,1),SESC(:,11),'OK')
plot(ADF(:,1),ADF(:,11),'OR')
plot(SHSC(:,1),SHSC(:,11),'*K')
plot(SHSC(:,1),SHSC(:,11),'OK')
xlabel('Ellipse area')
ylabel('Average value of the load voltage')
legend('IDF (class 1)','SEF (class 2)','ADF (class 3)','PDF (class 4)','SHF
(class 5)')
axis([0 1000 -2.5e-3 20e-4])
%__________________________________________________________________________

figure11 = figure('Color',[1 1 1]);
plot(IDF(:,1),IDF(:,12),'+')
hold on
```

```
plot(SESC(:,1),SESC(:,12),'OK')
plot(ADF(:,1),ADF(:,12),'OR')
plot(PDF(:,1),PDF(:,12),'O')
plot(SHSC(:,1),SHSC(:,12),'*K')
xlabel('Ellipse area')
ylabel('Root mean square value of the load voltage')
legend('IDF (class 1)','SEF (class 2)','ADF (class 3)','PDF (class 4)','SHF
(class 5)')
axis([0 1000 0 15])
%_________________________________________________________________________

figure12 = figure('Color',[1 1 1]);
plot(IDF(:,1),IDF(:,13),'+')
hold on
plot(SESC(:,1),SESC(:,13),'OK')
plot(ADF(:,1),ADF(:,13),'OR')
plot(PDF(:,1),PDF(:,13),'O')
plot(SHSC(:,1),SHSC(:,13),'*K')
axis([0 1000 0 15])
xlabel('Ellipse area')
ylabel('Average of the absolute value of the load voltage')
legend('IDF (class 1)','SEF (class 2)','ADF (class 3)','PDF (class 4)','SHF
(class 5)')
```

PUBLICATION OUT OF THIS THESIS

1. Ahmed S. Abd El-Hamid, and Rania M. Sharkawy, “Abnormality Diagnosis in Transformer Winding by Online Technique Using Circuit Model," ENGINEERING RESEARCH JOURNAL FACULTY of ENG. SHOUBRA, vol. 23, pp. 1–10, Jan. 2015.

2. Rania M. Sharkawy, Eman Beshr, Ahmed S. Abd El-Hamid, “LVQ Neural Network for Identification of Abnormal Conditions within Transformers” (accepted for publication in UPEC2015 IEEE conference)

ملخص الرسالة

في الآونة الأخيرة، محولات الكهرباء تعد من بين أهم الأصول المهمة جدا لشركات الكهرباء في نظام الطاقة. الطريقة المثلى لتشخيص حالة المحول هى تحليل استجابة التردد (FRA) حيث يتم بهذه الطريقة الكشف عن التشوهات الميكانيكية داخل المحول. تحديد استجابة التردد لأي محول يمكن أن تنفذ بواسطة خصائص المواد المصنع منها المحول. يمكن اعتبار تحليل استجابة المحول كبصمة اصبع بالنسبة للمحول . العيب الرئيسي لتحليل استجابة المحول، بالإضافة إلى كونها تحتاج الى فصل مصدر التيار عن المحول، هى ايضا طريقة تعتمد على تحليل الرسوم البيانية. لذلك هذا يتطلب خبير لتحليل هذه النتائج لإظهار وجود اى فشل في لفات المحولات. وبالتالي، هذا يزيد من حاجتنا إلى طريقة جديدة للمراقبة المستمرة بدون قطع مصدر التيار عن المحول وهذا لتقييم الحالة الداخلية له.

هذه الرسالة تقدم تقنية جديدة لكشف العيوب الداخلية داخل المحول بدون فصل مصدر التيارعن المحول وهذا عن طريق رسم العلاقة البيانية (ΔV- I_{in}) . تكمن ميزة هذة التقنية فى استخدام اجهزة القياس الموجودة على اى محول لمراقبة الفولت الداخل والخارج من المحول بالاضافة الى التيار الداخل للمحول. وبالتالى يمكن استخدامها كتقنية للمراقبة المستمرة بدون قطع مصدر التيار. اى تشوة او ازاحة فى لفات المحول يمكن ان يحدث تغيير فى معايير الدائرة وبالتالى تغيير فى استجابة التردد. هذه التغييرات يمكن الكشف عنها بواسطة التقنية المقترحة. هذه التقنية تحتاج الى مرجعية فى الاستجابه التى تتولد اثناء بدء تشغيل المحول للكشف عن هذه التغيرات.

الغرض من هذه الرسالة يمكن تقسيمة لقسمين. القسم الاول هو المحاكاة والتمييز بين عدة انواع مختلفة من تلف العزل. القسم الاخر هو تصنيف نوع التلف وتحديد مكانة فى لفات المحول طبقا لتقنيات الذكاء. ولتحديد هذه الاهداف تم تمثيل نموذج للفات المحول على برنامج (PSIM) وتم تنفيذ خمس انواع من تلف العزل التى يمكن ان تحدث فى لفات المحول على هذا النموذج وتتبع هذه الدراسه بتصميم مصنف شبكات عصبية وادراج بعض السمات المستخرجة اليه لتدريب الشبكة العصبية لتعطى اعلى كفاءة تصنيف.

وقد اظهرت النتائج ان التقنية المستخدمه فى التصنيف نجحت فى التعرف على نوع الفشل من بين خمس انواع مختلفة من فشل العزل وايضا تحديد مكانه خلال (4.55%) من الطول الكلى لللفات بدقة مقبولة تقدر بحوالى (98.1818%).

الاكاديمية العربية للعلوم و التكنولوجيا والنقل البحرى
كلية الهندسة و التكنولوجيا
قسم الهندسة الكهربية والتحكم

تطبيق التقنيات الذكية لتحديد الحالات الغير مرغوب فيها داخل المحولات

رسالة الماجيستير

مقدمة من:

مهندس / أحمد سيد عبد الحميد عوض

للحصول على درجة الماجيستير فى الهندسة الكهربية و التحكم

تحت إشراف

أستاذ دكتور / رانيا متولى الشرقاوى
مشرف

لجنة التحكيم

أستاذ دكتور /محمد عبد الرحيم بدر
ممتحن

أستاذ دكتور /ياسر جلال
ممتحن

القاهرة 2015

الاكاديمية العربية للعلوم و التكنولوجيا والنقل البحرى
كلية الهندسة و التكنولوجيا
قسم الهندسة الكهربية والتحكم

تطبيق التقنيات الذكية لتحديد الحالات الغير مرغوب فيها داخل المحولات

رسالة الماجيستير

مقدمة من:

مهندس / أحمد سيد عبد الحميد عوض

للحصول على درجة الماجيستير فى الهندسة الكهربية و التحكم

تحت إشراف

أستاذ دكتور / رانيا متولى الشرقاوى
قسم القوى الكهربية و التحكم
كلية الهندسة
الاكاديمية العربية للعلوم و التكنولوجيا والنقل البحرى

القاهرة 2015